This chapter is based on

3 Comparative proteomic profiling of human osteoblast-derived extracellular matrices identifies proteins involved in mesenchymal stromal cell osteogenic differentiation and mineralization

Marta Baroncelli[1], Bram C.J van der Eerden[1], Yik-Yang Kan[1], Rodrigo D.A.M Alves[1], Jeroen A.A Demmers[2], Jeroen van de Peppel[1], Johannes P. T.M van Leeuwen[1,*]

[1]Department of Internal Medicine, and [2]Proteomics Center, Erasmus University Medical Center, Wytemaweg 80, 3015 CN, Rotterdam, The Netherlands

J Cell Physiol. 2017; 9999:1–9. doi: 10.1002/jcp.25898

ABSTRACT

The extracellular matrix (ECM) is a dynamic component of tissue architecture that physically supports cells and actively influences their behavior. In the context of bone regeneration, cell-secreted ECMs have become of interest as they reproduce tissue-architecture and modulate the promising properties of mesenchymal stem cells (MSCs). We have previously created an *in vitro* model of human osteoblast-derived devitalized ECM that was osteopromotive for MSCs. The aim of this study was to identify ECM regulatory proteins able to modulate MSC differentiation to broaden the spectrum of MSC clinical applications. To this end, we created 2 additional models of devitalized ECMs with different mineralization phenotypes. Our results showed that the ECM derived from osteoblast-differentiated MSCs had increased osteogenic potential compared to ECM derived from undifferentiated MSCs and non-ECM cultures. Proteomic analysis revealed that structural ECM proteins and ribosomal proteins were upregulated in the ECM from undifferentiated MSCs. A similar response profile was obtained by treating osteoblast-differentiating MSCs with Activin-A. Extracellular proteins were upregulated in Activin-A ECM, whereas mitochondrial and membrane proteins were downregulated. In summary, this study illustrates that the composition of different MSC-secreted ECMs is important to regulate the osteogenic differentiation of MSCs. These models of devitalized ECMs could be used to modulate MSC properties to regulate bone quality.

Key words: Activin-A, bone regeneration; extracellular matrix; mesenchymal stromal cells

INTRODUCTION

The extracellular matrix (ECM) is an essential component of tissue architecture that provides structural and mechanical support to the cells. It is present in all tissues and has a rich tissue-specific composition of fibrous proteins, proteoglycans and water [1, 2]. These bioactive molecules are responsible for signaling processes that actively modulate cell behavior through cell/matrix interactions to maintain tissue homeostasis [3-5]. For instance, in the context of skeletal tissue, bone ECM is secreted by osteoblasts differentiated from mesenchymal stromal cells (MSCs), which secrete and mineralize the surrounding ECM, giving structural support to the skeletal tissue and regulating cellular processes to maintain bone integrity [6-8]. Thus, the peculiar composition of bioactive molecules makes the ECM far from being an inert cellular support [1].

During the recent years native tissue-derived ECMs have become increasingly popular as bioinstructive scaffolds for bone tissue engineering applications, in combination with biomaterials and MSCs [9, 10], which are promising candidates for cell-based regenerative therapies, due to their ability to differentiate toward osteoblasts and to secrete trophic factors [11, 12]. Cell-secreted ECMs have recently emerged in this context, as they reproduce to some extent the physiological tissue architecture, modulate stem cell properties and survival, and they aim to improve the structural functions of scaffold materials that are used for clinical applications [13-15]. Though the mechanical properties of cell-derived ECMs are poorer than the tissue-derived ECMs, they are readily available compared to tissues and organs, and they can be highly customized [13, 14]. We and others have already shown that osteoblast-derived ECMs improve *in vitro* cell-adhesion, proliferation, but especially the osteogenic potential of MSCs, due to the ECM specific proteomic composition that closely resembled human bone proteome. The proteomic components are the key modulators of MSC proliferation and osteogenic differentiation [16-18]. Moreover, MSC-secreted ECMs have been shown to improve culture conditions for *ex-vivo* expansion of MSCs, by maintaining MSC stem cell-properties and preventing loss of differentiation potential [19-21]. *In vitro* cell-secreted ECMs produced by MSCs at different stages of differentiation, have been shown to differentially affect the osteogenic potential of MSCs and therefore represent useful tools to study the role of ECM during tissue development [22].

Due to the role of the ECM on actively modulating MSC osteogenic differentiation, and to the increasing interest of using MSCs for cell-based therapies, the aim of our study was to identify ECM proteins that are involved in osteoblast differentiation and mineralization making these proteins suitable candidates to control bone quality. To this end, we created *in vitro* ECM models with extremely different mineralization

phenotypes, in order to get more insights into the effect of the ECM composition on MSC behavior. We have previously created an *in vitro* model of human MSC-secreted devitalized ECM from a mineralizing condition, that promoted the osteogenic differentiation of MSCs (Baroncelli M. *et al*, submitted). We thus modified the composition of the ECM by culturing MSCs without osteogenic inducers, resulting in an ECM from a non-mineralizing condition. Moreover, we took advantage of our previous findings on Activin A-mediated inhibition of osteoblast mineralization [23]. As we showed that Activin-A alters ECM-related genes, eventually leading toward the deposition of a matrix that is unable to mineralize [24], we generated an ECM from osteogenic MSCs treated with Activin-A (Activin-A ECM). The impact on osteogenic differentiation of MSCs and the composition of the different ECMs was compared by mass spectrometry to identify ECM components that enhance MSC-mediated mineralization.

MATERIALS AND METHODS

Cell culture and ECM preparations

Human bone marrow-derived MSCs were used to produce the devitalized ECM as previously described (Baroncelli M. *et al*, submitted). Briefly, commercially available MSCs (PT-2501, Lonza, Walkersville, MD, USA) from a single donor at passage 7, were cultured in growth media (alpha-Mem phenol-red free (GIBCO, Paisley, UK), 10% fetal bovine serum) for 2 days. Then, MSCs were cultured for 11 days by supplementing the growth medium with 100 nM dexamethasone and 10 mM β glycerophosphate (Sigma, St. Louis, MO, USA) to induce the osteogenic differentiation. MSCs were devitalized before the onset of mineralization by freeze-thaw cycles and DNAse treatment (10 U/ml; Sigma-Aldrich, St Louis MO, USA), followed by extensive washings with Phosphate Buffer Saline (PBS, Gibco BRL, Carlsbad, CA, USA) and sterile air drying, before freezing and subsequent use.

In parallel, MSCs were cultured with β-glycerophosphate but in the absence of dexamethasone to produce the non-mineralizing ECM. Activin A-ECM was deposited by culturing MSCs in osteogenic conditions, and adding Activin-A (25 ng/ml; R&D System, Minneapolis, MN, USA), following the same devitalization procedure. A schematic flowchart of the culture conditions is represented in Supplementary Figure 1. Throughout the remainder of this study we refer to the various generated ECMs as follows: 1) ECM obtained from the mineralizing condition as: min-ECM, 2) ECM obtained from the non-mineralizing condition as: nonmin-ECM, and 3) ECM obtained from the Activin A-treatment condition as: activin-ECM (Supplementary Figure 1A).

Culture of MSCs on ECMs and analysis of osteogenic differentiation

In order to check how the different ECMs affected MSC osteogenic potential, MSCs were cultured on the devitalized ECMs and on plastic, with osteogenic inducers in all the conditions (Supplementary Figure 1A). Alkaline phosphatase (ALP) activity was measured after 1, 6, 11 and 19 days of culture, and matrix mineralization at 6, 11 and 19 days of culture, as previously described [25] (Baroncelli M. *et al*, submitted).

Mass spectrometry analysis

The proteomic composition of the devitalized ECMs was analyzed by mass spectrometry (MS) with a label free quantification (LFQ) method, as previously described [26] (Baroncelli M. *et al*, submitted). Briefly, ECM samples were collected in PBS triton 0.1%, concentrated by centrifugal filters (Amicon Utra-0,5 ml centrifugal filters, Millipore; 3KDa cutoff), and quantified (BCA, Pierce Biotechnology, Rockford, IL, USA). Protein extracts (2.5 µg) in duplicate were reduced (NuPAGE® Reducing Agent), resolved by one-dimensional SDS-Page gel (NuPAGE®Novex® 4-12% Bis-Tris-Acetate Gels, Life technologies), and protein bands were stained with Coomassie staining (Bio-safe Coomassie, Bio-Rad, Hercules, CA, USA). Samples were processed for mass spectrometry and analyzed as previously described [26] (Baroncelli M. *et al*, submitted). Briefly, raw MS data were analyzed by using the MaxQuant Software (version 1.5.0.0) and Andromeda search engine, against the human proteome as provided by Uniprot database (taxonomy: *Homo sapiens*, release HUMAN_2013_04) (uniprot.org, v2014_05). Samples were run in duplicates and then averaged for the analysis. LFQ values higher than zero were considered for further analysis. Heat map of the ECM protein compositions was generated by using Perseus 1.3.0.4 (Max Plank Institute of Biochemistry 2012). The protein compositions of the ECMs were analyzed by using DAVID Bioinformatic Resources v6.7, to investigate significantly enriched Gene Ontology (GO) terms [27]. The whole human genome was used as background and only significantly enriched GO terms (Benjamini $P < 0.05$) were considered. The 31 proteins not detected in min-ECM and the 149 detected only in this ECM were analyzed through QIAGEN's Ingenuity® Pathway Analysis (IPA®, QIAGEN Redwood City www.qiagen.com/ingenuity).

Statistical analysis

Data were representative of multiple independent experiments and all values were displayed as average ± standard deviation (SD) of biological replicates. Two-way analysis of variance (ANOVA), followed by Bonferroni Post Hoc test was used to calculate significance, otherwise indicated elsewhere.

RESULTS

Min-ECM increased matrix mineralization by MSCs compared to nonmin-ECM and activin-ECM

To check if the ECM composition modulated the osteogenic potential of MSCs, cells were differentiated on the three different types of ECMs and on plastic. Osteogenic differentiation and matrix mineralization were accelerated when MSCs were cultured on min-ECM compared to plastic, as shown in Figure 1A and 1B, and confirming our previous findings (Baroncelli M. *et al*, submitted). Matrix mineralization by MSCs on min-ECM was more than 15-fold higher than on plastic at day 19 of culture, as assessed by calcium deposition (Figure 1B).

Figure 1A shows a significantly increased ALP activity in MSCs cultured on any of the ECMs than on plastic after 6, 11 and 19 days of culture. Unexpectedly, MSCs cultured on nonmin-ECM showed 4-fold higher levels of ALP activity than MSCs on min-ECM at day 19 of culture (P<0.001, Figure 1A). Despite this, matrix mineralization by MSCs cultured on min-ECM was significantly higher than on nonmin-ECM at day 19 of culture (4-fold at day 19 of culture, P<0.001).

Activin-A was previously shown to inhibit matrix mineralization of human osteoblast cultures, by affecting the ECM composition [23, 24]. We treated osteogenic MSCs with Activin-A to create a devitalized activin-ECM. The ALP activity of MSCs cultured on activin-ECM showed similar level as MSCs on min-ECM at day 11 of culture, but was 3-fold higher after 19 days, like in MSCs on nonmin-ECM. However, matrix mineralization by MSCs cultured on min-ECM was more than 2-fold higher than cells grown on activin-ECM after 19 days of culture (P<0.001) (Figure 1B). Together, this illustrated that activin-ECM had a reduced matrix mineralization compared to

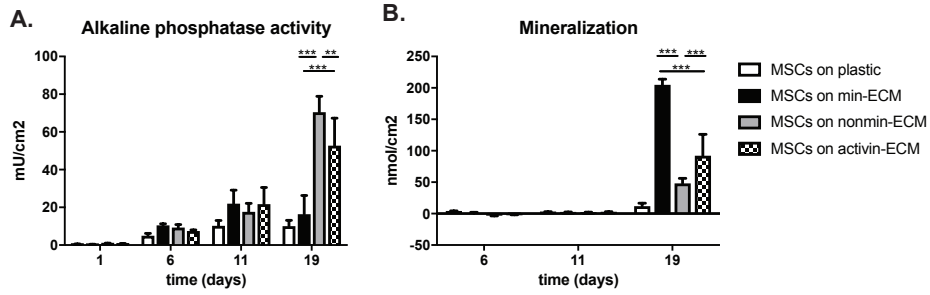

Figure 1. Min-ECM increased matrix mineralization by MSCs compared to nonmin-ECM and activin-ECM. A) ALP activity measured in MSCs cultured on plastic, min-ECM, nonmin-ECM and activin-ECM for 19 days. B) Calcium deposition by MSCs cultured in similar conditions at day 6, 11 and 19 of culture. The values of ALP activity and mineralization in MSCs on the different ECMs were subtracted by the contributions of the ECMs cultured without cells. The results were representative of multiple independent experiments (**, P<0.01; ***, P<0.001). Bars indicate Average ± SD.

min-ECM but still retained the ability to enhance the osteogenic differentiation, in line with our previous findings [24]. Overall the min-ECM increased the osteogenic potential of MSCs, compared to the other 2 ECM model we created. As MSCs on all three ECMs were cultured in identical osteogenic medium, the functional differences observed must result from different protein compositions of the ECMs.

Altered protein composition of nonmin-ECM compared to min-ECM

We analyzed the protein composition of the ECMs by comparative mass spectrometry of min-ECM and nonmin-ECM, to identify possible candidates underlying the different phenotypic effects on osteogenic MSCs. Figure 2A illustrates that we detected 767 proteins in the nonmin-ECM and 846 in the min-ECM. Of these, 554 proteins were shared between the 2 ECMs, while 213 proteins were detected only in nonmin-ECM and 292 uniquely in the min-ECM, highlighting differences in the ECM compositions. Besides the unique proteins, we focused on the proteins that had at least 2-fold difference in abundance between the 2 ECMs. Seventy-seven proteins were more than 2-fold upregulated in the nonmin-ECM (Figure 2B) and 74 were more than 2-fold downregulated (Figure 2C). For a more comprehensive analysis, we combined the unique proteins and the 2-fold different proteins. First, the 77 proteins that were more than 2-fold upregulated in the nonmin-ECM were added to the 213 unique ones in this ECM (Figure 2B) (complete list in Supplementary Table 1). As displayed in Figure 2D, the GO analysis of the resulting 290 proteins showed that these proteins were involved in ECM structure (GO:0031012) and cell-matrix adhesion (GO:0007160), with proteins such as Tenascin (TNC), Vitronectin (VTN), Fibronectin (FN1), Fibrillin 1 (FBN1) and Hyaluronan and proteoglycan link protein 1 (HAPLN1) (Supplementary Table 3). Moreover, growth factors known to modulate osteoblast behavior such as Transforming growth factor-beta-induced protein ig-h3 (TGFβI), Connective tissue growth factor (CTGF) and Cysteine-rich protein 61 (CYR61) were detected within the extracellular proteins in the nonmin-ECM, but also Insulin-like growth factor 2 (IGF2) and insulin-like growth factor-binding proteins (IGFBP5, IGFBP7) (Supplementary Table 1). Interestingly, translation (GO:0006414) was among the most significantly enriched GO terms and many ribosomal protein-subunits were detected in nonmin-ECM. Moreover, protease and peptidase inhibitors were also detected within the significantly enriched GO terms (regulation of proteolysis GO:0030162), as well as histones (nucleosome GO:0000786) (Supplementary Table 3).

Secondly, 74 proteins that were at least 2-fold downregulated in the nonmin-ECM were combined with the 292 proteins only detected in the min-ECM (Figure 2C; complete list in Supplementary Table 2). The GO analysis of the resulting 366 proteins indicated that significantly enriched GO terms were related to mitochondrial functions (mitochondrion GO:0005739), as shown in Figure 2D. Within this enriched

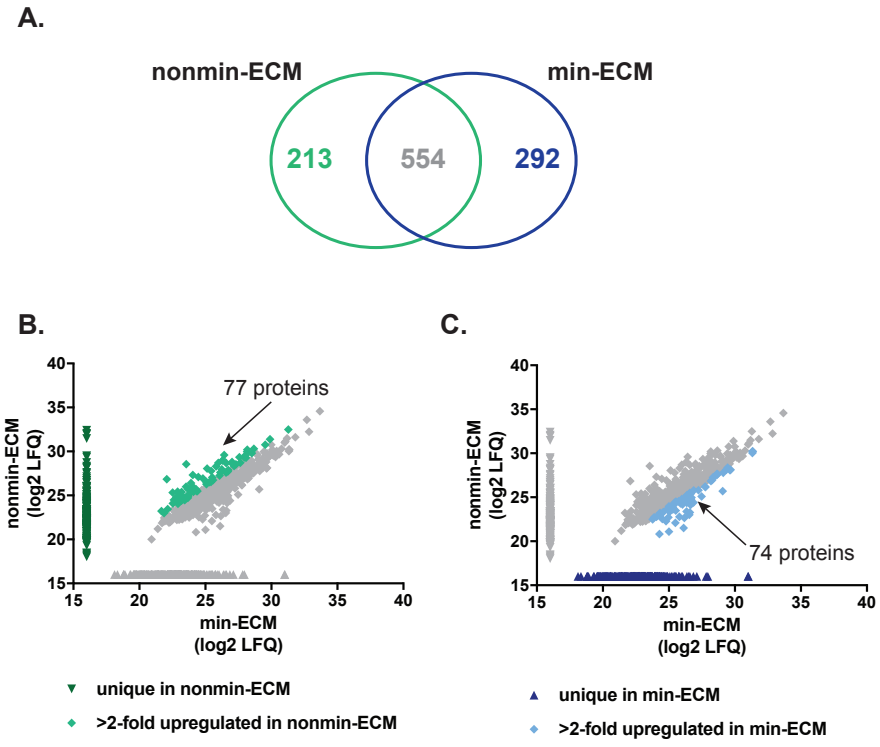

D.

GO term		Fold enrichment	
		nonmin-ECM	min-ECM
GO:0006414	translational elongation	**22.96**	0.00
GO:0030162	regulation of proteolysis	**9.38**	0.00
GO:0007160	cell-matrix adhesion	**6.82**	0.00
GO:0000786	nucleosome	**6.20**	0.00
GO:0031012	extracellular matrix	**2.97**	0.91
GO:0005739	mitochondrion	0.90	**4.10**
GO:0016192	vesicle-mediated transport	0.86	**2.12**
GO:0005509	calcium ion binding	1.71	**1.87**

Figure 2. Comparative protein profiling of nonmin-ECM and min-ECM. A) 213 proteins were detected only in nonmin-ECM, 554 proteins were shared, and 292 were detected only in min-ECM. B) Scatter plots of proteins detected in nonmin-ECM versus min-ECM: 77 proteins were more than 2-fold upregulated in nonmin-ECM than in min-ECM (light green); 213 proteins detected only in the nonmin-ECM (dark green). C) 74 proteins were more than 2-fold upregulated in nonmin-ECM than in min-ECM (light blue); 292 proteins detected only in min-ECM (dark blue). In both cases, colored proteins were considered for further GO analysis. D) GO analysis of the resulting 290 proteins upregulated in the nonmin-ECM and the 366 proteins upregulated in the min-ECM. Bold: significantly enriched GO terms (Benjamini P <0.05).

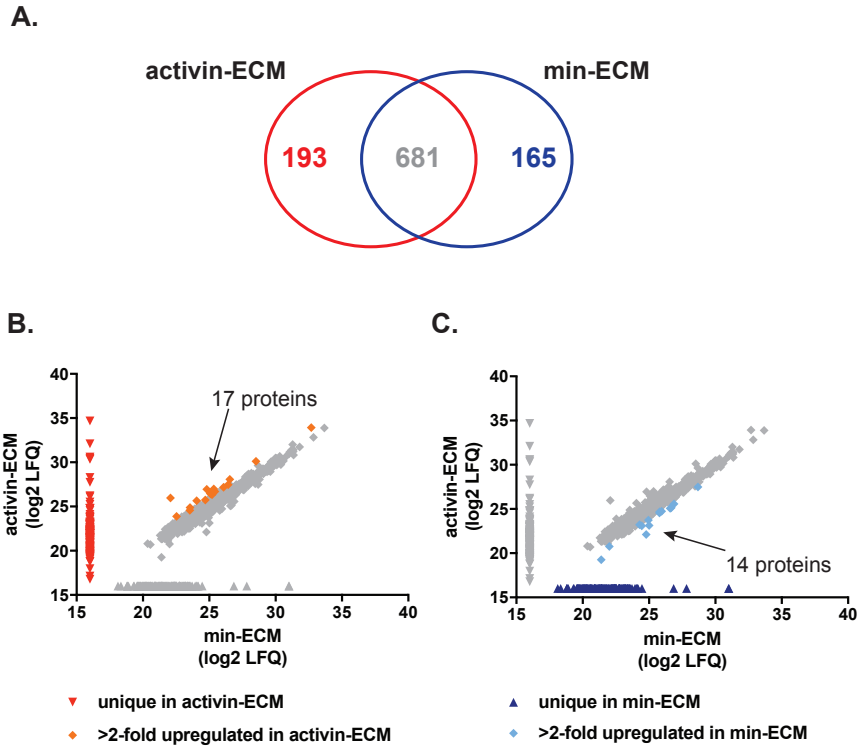

D.

GO term		Fold enrichment	
		activin-ECM	min-ECM
GO:0030414	peptidase inhibitor activity	**6.88**	0.00
GO:0005198	structural molecule activity	**3.74**	0.00
GO:0005739	mitochondrion	**2.29**	**3.34**
GO:0044421	extracellular region part	**2.15**	0.77
GO:0031090	organelle membrane	**1.94**	**2.93**

Figure 3. Comparative protein profiling of activin-ECM and min-ECM. A) 193 proteins were detected only in the activin-ECM, 681 proteins were shared with the min-ECM, and 168 were detected only in min-ECM. B) 17 proteins were more than 2-fold upregulated in activin-ECM than in min-ECM (orange); 193 proteins were detected only in the activin-ECM (red). C) 14 proteins were more than 2-fold upregulated in min-ECM than in activin-ECM (light blue); 168 proteins were detected only in min-ECM (dark blue). Colored proteins were considered for further analysis. D) GO analysis of the resulting 210 proteins upregulated in activin-ECM and the resulting 165 proteins upregulated in min-ECM. Bold: significantly enriched GO terms (Benjamini P <0.05).

GO term, we detected antioxidant proteins such as Superoxide dismutase 1 and 2 (SOD1, SOD2) and Catalase (CAT), revealing important effect of the devitalized ECM on the cultured cells (Supplementary Table 3). The GO term 'calcium ion binding GO:0005509' was also significantly enriched, with proteins such as Anoctamin 6 (ANO6) and annexins (ANXA5, ANXA6, ANXA7, ANXA11) (Supplementary Table 3), which are calcium-binding proteins and known mediators of mineralization [28, 29]. Along with this finding, Alkaline phosphatase was also downregulated in the nonmin-ECM (Supplementary Table 2).

Comparative protein profiling of activin-ECM and min-ECM

We analyzed the protein composition of activin-ECM and compared this to the proteins identified in the min-ECM. We detected 874 proteins in activin-ECM, as shown in Figure 3A. The 2 ECMs shared 681 proteins, and 193 were detected only in activin-ECM, whereas 165 proteins only in the min-ECM. Like for the nonmin-/min-ECM comparison we also focused on the 2-fold different proteins. In activin-ECM compared to min-ECM, 17 and 14 proteins were 2-fold upregulated and downregulated, respectively (Figure 3B and C). The most abundant protein detected in the activin-ECM was BMP2 inducible kinase (BMP2K) (Supplementary Table 4), which was shown to impair osteoblast differentiation *in vitro* [30]. Seventeen proteins were more than 2-fold upregulated in activin-ECM; to these, we added the 193 proteins that were detected only in this matrix for further analysis (Figure 3B; complete list in Supplementary Table 4). The GO analysis of the resulting 210 proteins indicated that these were extracellular proteins with a structural function (extracellular region part GO:0044421, structural molecule activity GO:0005198), as shown in Figure 3D. Within these GO terms we detected Cartilage oligomeric matrix protein (COMP), Basement membrane-specific heparan sulfate proteoglycan core protein (HSPG2), but also Collagen alpha-1(XII) chain (COL12A1), and the growth factors CTGF and TGFβI (Supplementary Table 6). Peptidase inhibitor activity (GO:0030414) with proteins such as Fetuin B (FETUB), was one of the most enriched GO terms. Mitochondrial and membrane proteins were upregulated in activin-ECM (mitochondrion GO:0005739, organelle membrane GO:0031090), but interestingly these GO terms were significantly enriched also in the GO analysis of the 179 proteins upregulated in the min-ECM (165 detected only in this matrix, and 14 proteins that were more than 2-fold upregulated) (Supplementary Table 5). Extracellular region part (GO:0044421) was not within the significantly enriched GO terms, but still extracellular proteins were detected, such as Collagen alpha-1(III) chain (COL3A1) and Laminin subunit gamma-1 (LAMC1) (Supplementary Table 6). Overall we could demonstrate that Activin-A modified the ECM-composition to create a microenvironment that retained the ability of Activin-A to reduce the mineralization of osteoblast cultures.

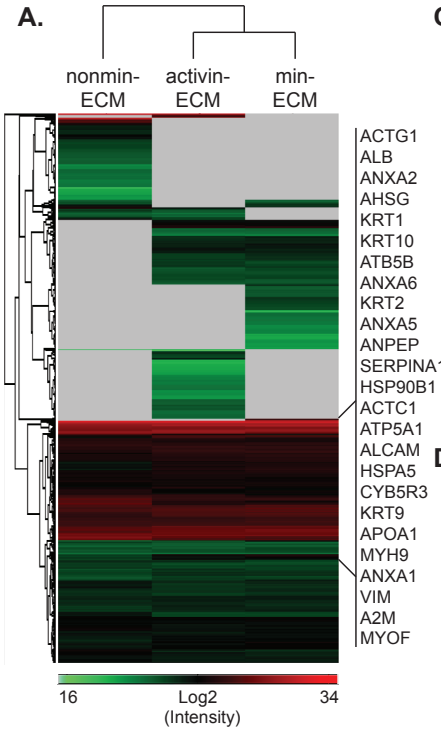

C.

GO term		fold enrichment	# proteins
GO:0016209	antioxidant activity	6.97	11
GO:0005200	structural constituent of cytoskeleton	6.84	17
GO:0006414	translational elongation	5.98	21
GO:0007160	cell-matrix adhesion	4.53	14
GO:0031982	vesicle	3.07	81
GO:0016477	cell migration	3.02	29
GO:0005739	mitochondrion	2.82	121
GO:0031012	extracellular matrix	2.13	29
GO:0005509	calcium ion binding	1.91	59

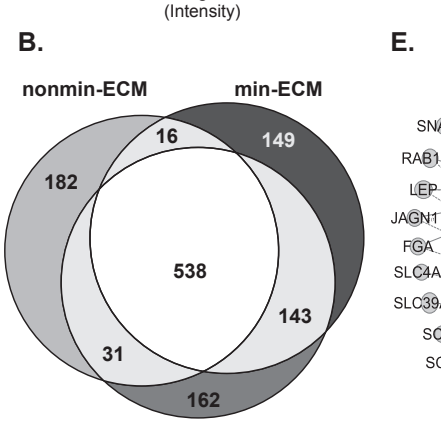

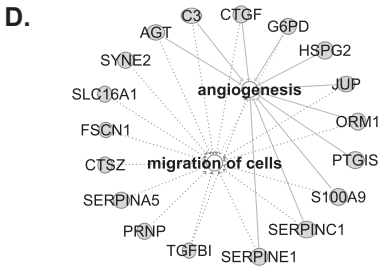

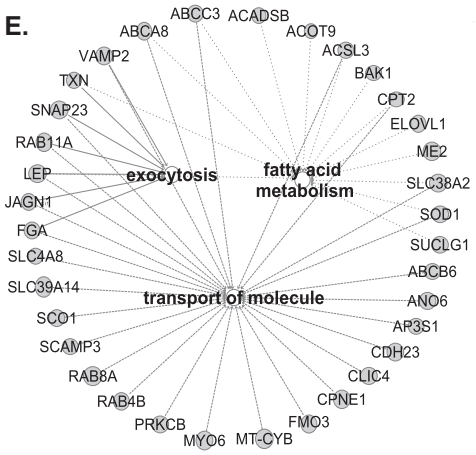

Figure 4. Comparative proteomic analysis of the 3 devitalized ECMs. A) Heat map of protein abundance (LFQ values) across the devitalized ECMs. The top 25 most abundant proteins detected in all the ECMs are indicated next to the heat map. Red: high abundance, green: low abundance; grey: not detected. B) Venn diagram indicating proteins present across the 3 devitalized ECM. C) GO analysis of the 538 shared proteins. D) Ingenuity Pathway Analysis of the 31 proteins not detected in the min-ECM. 'Angiogenesis' (P=8.35 E-08) and 'migration of cells' (P=2.31 E-07) were within the most enriched pathways. E) IPA analysis of the 149 proteins detected only in the min-ECM. Exocytosis (P=8.57 E-04), 'Fatty acid metabolism' (P=9.42 E-04), 'Transport of molecule' (P=1.22 E-03), were within the top 30 most enriched terms (P<1 E-04).

Three-way comparison of ECMs

Eventually, we compared the protein composition of all the 3 ECMs together. The proteins shared by the 3 ECMs contained the most abundant ones (the top 25 most abundant proteins detected in all the 3 ECMs are shown in Figure 4A). Hierarchical cluster analysis showed a higher similarity between activin-ECM and min-ECM, than nonmin-ECM (Figure 4A). The 3 ECMs shared 538 proteins, as shown in Figure 4B (complete list in Supplementary Table 7). GO analysis of these 538 proteins indicated that they were involved in mitochondrial functions, as shown in Figure 4C by the significantly overrepresented processes (antioxidant activity GO:0016209, ATP metabolic processes GO:0046034, mitochondrion GO:0005739). Furthermore, GO terms such as structural constituent of cytoskeleton (GO:0005200) and plasma membrane part (GO:0044459) were significantly enriched. Extracellular matrix GO term (GO:0031012) was significantly enriched, confirming the validity of freeze-thaw cycles as treatment to obtain cell-secreted ECMs. The proteins shared by the ECMs were involved also in cell-matrix adhesion and migration (GO:0007160, GO:0016477). 'Calcium ion binding' (GO:0005509) and 'vesicle' (GO:0031982) were also significantly enriched GO terms, with proteins such as annexins, Thrombospondin (THBS1) and Osteonectin (SPARC) (complete list in Supplementary Table 8), highlighting a possible role in matrix-vesicle-driven mineralization. With the aim to identify negative regulators of mineralization, we analyzed the 31 proteins that were present in both nonmin-ECM and activin-ECM but absent in min-ECM (Figure 4B; complete list in Supplementary Table 9). Ingenuity Pathway Analysis revealed that 12 of these proteins were involved in angiogenesis and 16 in cell migration (Figure 4D), most of them stimulating these pathways. Within these proteins we detected serpins, Cathepsin Z (CTSZ) and other extracellular proteins such as HSPG2. In addition, growth factors such as TGFβI and CTGF, were detected in these ECMs but not in min-ECM. No known inhibitors of mineralization were detected within these 31 proteins.

We analyzed the 149 proteins detected only in min-ECM (Figure 4B; complete list in Supplementary Table 10) by IPA, with the aim to find promotors of mineralization, as this process on min-ECM was quicker than on activin-ECM and nonmin-ECM. IPA revealed that there were no significantly enriched terms directly related to mineralization, but these proteins were related to exocytosis (P=8.57 E-04), as shown in Figure 4E. Moreover, there were cytoplasmic proteins such as SOD1 involved in fatty acid metabolism (P=9.42 E-04) and transport of molecule (P=1.22 E-03). Other mitochondrial proteins were also present, but not interconnected with the proteins involved in the other selected terms.

DISCUSSION

In the current study, we performed a comparative analysis of three ECMs that reflected two extremely different phenotypes with respect to mineralization. We identified 149 proteins that were uniquely present in the min-ECM and 31 proteins that were detected in both the nonmin- and activin-ECM but absent in the min-ECM. Interestingly, the set of 31 proteins did not contain known inhibitors of mineralization. Within these proteins there were growth factors and proteins linked to cell migration and angiogenesis. In our view, this implicates that the role of these shared ECM-proteins is more directed toward regulating cell function and bone formation-related processes such as angiogenesis, than primarily directly affecting mineralization.

We have previously shown that the devitalized ECM produced by human MSCs in osteogenic conditions was osteopromotive (Baroncelli M. *et al*, submitted). In this study, we showed that this min-ECM accelerated the matrix mineralization by MSCs compared to ECM produced by MSCs cultured without osteogenic inducers and in the presence of Activin-A. Our findings showed that matrix mineralization started first by MSCs cultured on min-ECM, then on activin-ECM, followed by nonmin-ECM, and eventually on plastic. Accordingly, ALP activity was expected to be lower in cells cultured on nonmin- and activin-ECM than on min-ECM, but this was not the case at later stages of culture. This is most likely explained by the fact that we missed the peak in ALP in min-ECM condition by only measuring ALP at a limited number of days, whereas in nonmin- and activin-ECM condition the peak of ALP was delayed to day 19 (schematic representation Supplementary Figure 1B). Moreover, cells on min-ECM might need less ALP as the ECM is half-build. Nevertheless, the major end-point mineralization, which is cumulative in time, was clearly different between the min-ECM and the two other ECMs, demonstrating that ECM plays a key role in modulating the osteogenic potential of MSCs. As MSCs on all types of ECMs were cultured in the same osteogenic conditions, the phenotypic differences were caused by the different composition of the ECMs they were cultured on. We focused on the protein composition of the three ECMs. Most of the proteins were shared between the three ECMs and they were involved in ECM structure, therefore the differences in culture conditions during the generation of the ECMs did not lead to an overall major change in protein composition. For example, about 64% of the proteins in the min-ECM were also present in the other two ECMs. Despite this, still differences in the ECM composition were responsible for acceleration in matrix mineralization. Indeed, extracellular proteins such as Alpha-2-HS-glycoprotein (AHSG) or Fetuin A, and FETUB, but also the plasma-membrane protein Ectonucleotide pyrophosphatase/phosphodiesterase family member 1 (ENPP1), that are all known to negatively

regulate matrix mineralization by different mechanisms [31-33], were detected in nonmin-ECM. Surprisingly, proteins such as FN1, VTN and TNC, which are known to promote adhesion and osteogenic differentiation of MSCs [34-36], were detected as upregulated in the nonmin-ECM. The presence of inhibitors of mineralization therefore should dominate the effect of the promotors of MSC adhesion and differentiation, as the nonmin-ECM had reduced matrix mineralization by MSC compared to min-ECM. Indeed, proteins such as annexins and ALP, which are known promotors of osteogenic differentiation [29, 37], were downregulated in the nonmin-ECM. It is intriguing that MSCs cultured without dexamethasone were anyway producing a matrix that contained promotors of osteogenic differentiation. Our findings confirm previous studies, in which a stem cell matrix produced by undifferentiated MSCs was shown to inhibit osteogenesis of MSCs [22], and it was proposed as *in vitro* tool to study osteogenesis, implementing the use of cell-secreted matrices to investigate tissue development. Interestingly, many ribosomal proteins were detected in the nonmin-ECM, meaning that a high translational activity was ongoing in the MSCs that were producing the ECM, and these proteins stick to the ECM despite the extensive washings. Due to the role of ribosomal proteins in healthy bone, nonmin-ECM could be used to study how the microenvironment affects cell behavior physiologically, but also pathologically, to gain further insights in the niche-induced oncogenesis, e.g. in the case of ribosomopathies, in which alterations of bone marrow-stroma have been shown to be critical for the pathogenesis [38, 39]. Growth factors such as TGFβI and CTGF were detected in both nonmin-ECM and activin-ECM at the moment of the devitalization, but surprisingly they were not detected in min-ECM. Cell-secreted ECMs have been shown to sequester growth factors, making these ECMs a more suitable microenvironment for stem cells to maintain their osteogenic potential during *ex-vivo* expansion [18-20]. Therefore, it would be interesting to investigate the effect of the nonmin-ECM to enhance the expansion of MSCs during *ex-vivo* cultures, to increase the amount of MSCs for clinical applications, as already hypothesized for other models of cell secreted ECMs [19, 20] or also the effect of this ECM on MSC differentiation toward other lineages.

MSCs cultured on min-ECM showed an accelerated mineralization than MSCs on activin-ECM. We previously have shown that Activin-A strongly reduces osteoblast mineralization, and in the current study that the ECM produced by MSCs treated with Activin-A still retained this ability [23, 24]. Even with a different devitalization treatment to produce the ECM, we were still able to confirm our previous findings. Despite the functional effect, the protein composition of activin-ECM was more similar to the min-ECM than to the nonmin-ECM, and this was most likely due to the presence of dexamethasone in culture medium of both conditions. Extracellular proteins involved in ECM structure such as COMP, HSPG2, Fibulin 2 (FBLN2) and

COL12A1 were upregulated in activin-ECM than in min-ECM. HSPG2 or Perlecan is a proteoglycan important in cartilage and bone development, but also in modulating growth factors availability [40, 41], whereas COL12A1 is known to promote osteogenic differentiation of osteoblasts [42], in contrast with our findings. However, COL12A1 was also the highest upregulated protein in MSCs treated with Activin-A [24]. Our findings confirmed our previous studies, that Activin-A changes the expression profile of ECM genes and proteins in osteoblasts [23, 24]. Activin-A might play a critical role in modulating the ECM composition, by stimulating the ECM secretion at the early stages of osteogenic differentiation, but resulting in a quite immature ECM that is unable to support the final stages of mineralization.

The proteins that were upregulated in min-ECM were related to mitochondrial functions. These proteins might be related to energy metabolism functions and most likely derive from lysis of the ECM-secreting MSCs. This fits the fact that MSCs treated with osteogenic inducers during matrix deposition, are metabolically highly active, as the osteogenic differentiation is a high energy demanding process. Within the 149 proteins detected uniquely in min-ECM there were cytoplasmic proteins involved in exocytosis, a process related to matrix vesicle shedding. Despite this, we were not able to identify specific osteogenic inducers to be strikingly abundant in min-ECM, making us conclude that is more the overall composition of the ECMs, i.e. the combination of ECM proteins and balance between stimulators and inhibitors, that is responsible for the differential behavior of the cells and for the effect on mineralization. For instance, ALP but also Annexins, were present in the three ECMs, but maybe they were more functional in the min-ECM. Moreover, proteins that were not detected in min-ECM were involved in angiogenesis and migration, making us conclude that probably the composition of the min-ECM is not directly influencing mineralization but it is important to regulate cell behavior.

In summary, we presented three models of MSC-derived ECM that were able to differentially modulate the osteogenic potential of MSCs due to their peculiar protein compositions. The regulatory proteins of these ECMs give useful insights in understanding how ECM influence MSC behavior for bone formation-related processes. The devitalized ECM derived by undifferentiated MSCs could be used as *in vitro* tool to study the different steps of bone tissue development, together with the devitalized ECM produced by MSCs in osteogenic conditions we previously developed. Activin-ECM gives further insights in the molecular mechanisms of Activin-A-driven reduction of mineralization, to develop Activin-A as potential target to for clinical applications. Together these cell-secreted ECMs could be used as useful tools to modulate the osteogenic potential of MSCs, to broaden their spectrum of clinical applications, and maybe use them to reduce ectopic calcification or unwanted mineralization to control bone formation and quality. Finally, the current study

provides interesting ECM protein candidates that need further functional analyses to modulate MSC behavior in a controlled manner.

ACKNOWLEDGEMENTS

This work was supported by a grant from the Dutch government to the Netherlands Institute for Regenerative Medicine (NIRM, grant No: FES0908) and Erasmus Medical Center.

The authors thank Molecular Medicine Post Graduate School, T. Strini, C. S. van der Leije and M. Koedam for technical support, and K. Bezstarosti and D. Dekkers for mass spectrometry analysis.

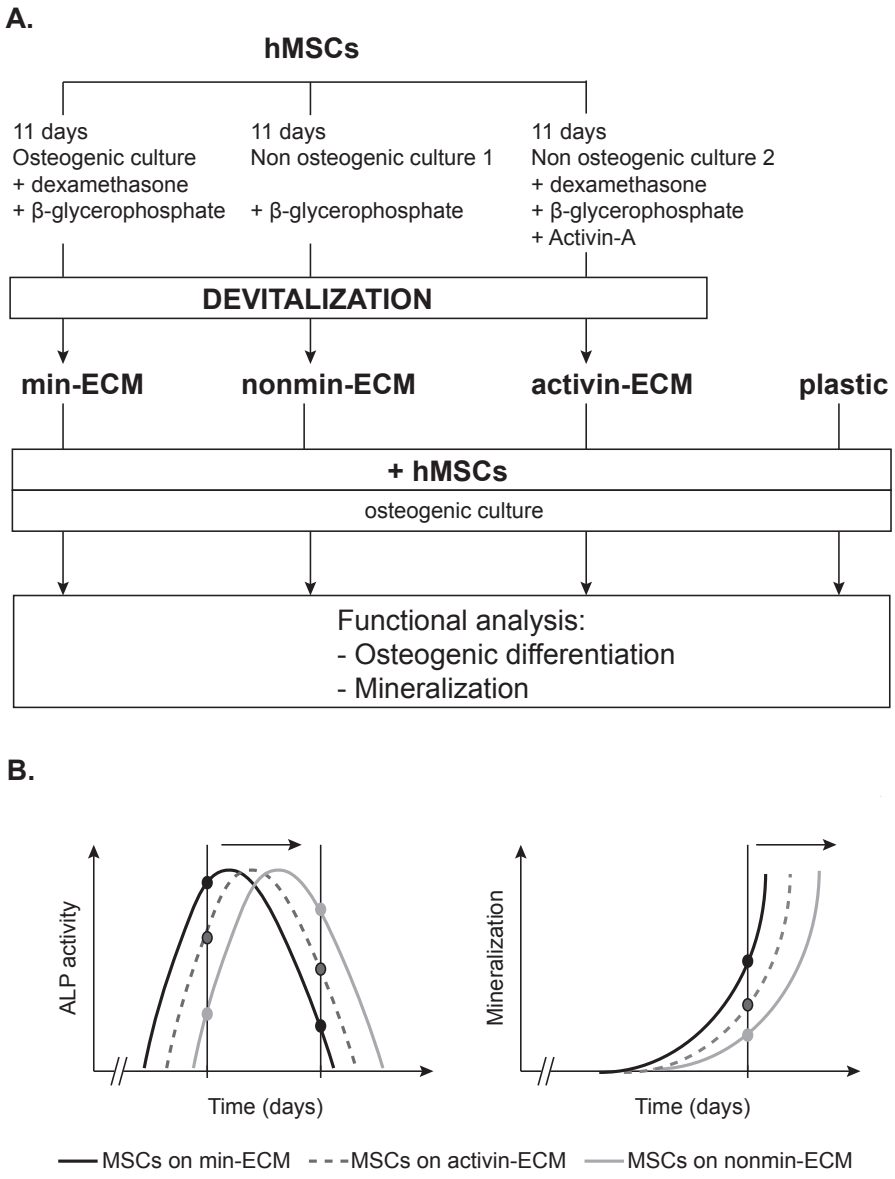

Supplementary Figure 1. A) Schematic overview of ECM preparation and culture conditions. B) Schematic model of osteogenic differentiation (peak of ALP activity) and mineralization over time. Matrix mineralization occurred first on min-ECM, then on activin-ECM and eventually on nonmin-ECM.

Supplementary Table 1. List of proteins detected by mass spectrometry only in the nonmin-ECM and more than 2-fold upregulated in nonmin-ECM compared to min-ECM. Proteins are indicated as Protein IDs and ranked for abundance in nonmin-ECM. Color scale represents high difference in abundance between the ECMs (LFQ values).

Protein ID	LFQ nonmin-ECM	LFQ min-ECM	ratio
CON__P12763	6014900000	2605800000	2.31
G3V5X4	5709600000	0	
Q562R1	4448800000	0	
REV__Q9Y4K1	4093900000	0	
Q7Z4T8	2977500000	0	
CON__P34955	2798000000	997520000	2.80
CON__P15497	1826900000	779530000	2.34
CON__ENSEMBL:ENSBTAP00000024146	1319400000	427310000	3.09
E9PIM6	1240500000	301310000	4.12
P24821-4	1058300000	299990000	3.53
CON__Q0IIK2	939990000	385210000	2.44
P62805	813250000	89920000	9.04
CON__Q3SX09	809290000	279230000	2.90
B7Z7M4	770280000	0	
CON__P01966	678790000	200620000	3.38
B1AN99	676600000	0	
P02751-17	674830000	259890000	2.60
P02545-2	652460000	283530000	2.30
Q99880	540920000	84729000	6.38
Q99878	522480000	82853000	6.31
P21589	466450000	136040000	3.43
P60709	450130000	0	
F8W1R7	439500000	210890000	2.08
Q92743	437440000	66197000	6.61
H0YD13	428960000	133390000	3.22
P19105	427870000	99731000	4.29
Q9Y6C2	392190000	12268000	31.97
P08195-2	389590000	167220000	2.33
P11279	340220000	152110000	2.24
F5H555	335520000	0	
CON__P17690	328830000	59061000	5.57
H0Y8D1	299000000	0	
Q15058	288720000	0	
CON__Q3ZBS7	279830000	36701000	7.62
Q71U36-2	261450000	79267000	3.30
Q6NZI2	246720000	111120000	2.22
CON__Q2KIS7	232270000	45432000	5.11
P30447	220720000	109630000	2.01
Q7L775	206320000	0	
Q12884	205310000	73866000	2.78

Protein ID	LFQ nonmin-ECM	LFQ min-ECM	ratio
P35232	203710000	99074000	2.06
P05121	186970000	0	
CON__ENSEMBL:ENSBTAP00000007350	167080000	17417000	9.59
Q9UKX5	161020000	71091000	2.26
Q8IYK2	147420000	0	
K7EMV3	144160000	23100000	6.24
Q5JP53	139430000	47999000	2.90
CON__Q3MHN5	128230000	29429000	4.36
CON__Q9N2I2	128160000	0	
CON__Q3T052	119660000	4428600	27.02
P08238	111260000	49905000	2.23
P62277	110700000	0	
M0QZQ8	108780000	0	
CON__Q9TRI1	97310000	44790000	2.17
CON__Q58D62	96771000	35301000	2.74
P04075	96216000	41254000	2.33
REV__B7Z1I8	94065000	0	
P54289-4	89175000	36802000	2.42
P07858	88925000	15689000	5.67
Q15582	88621000	0	
P39019	81093000	35432000	2.29
P35625	69377000	0	
Q2M3V2	68986000	0	
P18564-2	67464000	0	
K7ERI7	66695000	17378000	3.84
P62081	66439000	12143000	5.47
P80723	63699000	0	
CON__Q3SZH5	57415000	0	
P23396	55987000	13320000	4.20
P04632	55032000	15162000	3.63
P62269	54092000	20598000	2.63
Q969G5	53509000	18604000	2.88
O75531	51619000	18990000	2.72
E5RI99	50854000	18427000	2.76
Q8N257	48278000	0	
P69905	47594000	0	
P55290	47110000	21972000	2.14
O75487	46864000	21029000	2.23
P32969	45157000	7780700	5.80
CON__Q2UVX4	44973000	0	
CON__P01044-1	44558000	17840000	2.50
P24844	43847000	9629700	4.55
P29966	43230000	0	
Q7Z406	43047000	0	

Protein ID	LFQ nonmin-ECM	LFQ min-ECM	ratio
Q13683-9	42117000	6045900	6.97
I3L2P2	36770000	0	
P61158	35890000	13709000	2.62
CON__P81644	35679000	0	
Q6S8J3	34788000	0	
H3BN98	31794000	13449000	2.36
P07900	31024000	13438000	2.31
Q9UHI8	30317000	0	
P62851	30235000	8605100	3.51
Q16555	29936000	10328000	2.90
H7C2W9	29554000	0	
P01344	29470000	0	
Q9H4G4	28956000	7317100	3.96
O15144	27731000	13358000	2.08
P05976-2	27689000	0	
P04156-2	27450000	0	
Q16647	26280000	0	
P30483	26169000	11944000	2.19
H0Y984	25606000	0	
P10321	24662000	10367000	2.38
Q01650	24520000	8919600	2.75
REV__Q9NTI5-2	24016000	0	
CON__Q03247	23682000	6444100	3.67
P05386	23447000	0	
P62750	23238000	11341000	2.05
P17655	22810000	0	
Q5JTV8	22311000	9566300	2.33
P62906	22168000	8800200	2.52
P27487	21688000	0	
P19320-2	21429000	0	
O95865	21117000	0	
P61160	20085000	8489400	2.37
P00846	19971000	0	
Q9Y613	19794000	0	
P24593	19044000	0	
Q9Y617	18513000	0	
P62263	18052000	0	
CON__Q3Y5Z3	17801000	6059800	2.94
REV__H0Y390	17632000	0	
P51970	17475000	7976000	2.19
B4E241	17454000	0	
P07195	17349000	0	
P22413	17060000	0	
P10915	16657000	0	

Protein ID	LFQ nonmin-ECM	LFQ min-ECM	ratio
REV__Q9H2G2-2	15897000	0	
P27449	15098000	0	
Q15393	14687000	0	
O14684	14179000	0	
P61353	13733000	0	
O15145	13579000	0	
P16403	12723000	0	
Q15404-2	11451000	4627300	2.47
K7EMS3	11196000	0	
S4R3I5	11006000	0	
O43324-2	10967000	0	
Q16658	10938000	0	
Q9Y625	10767000	0	
Q9NX14	10667000	0	
O00622	10513000	0	
P62701	10437000	0	
Q99584	9947700	0	
Q16270-2	9932900	0	
CON__P02777	9703100	3343000	2.90
P20930	9578200	0	
P29279	9471300	0	
Q9UBG3	9361000	0	
C9JAW5	9293500	0	
C9JD32	9269100	0	
Q71UI9-2	9205400	0	
P62847-2	9055800	0	
P37108	8985300	0	
B7Z2F4	8827100	0	
P67809	8620900	0	
C9JRA9	8588700	0	
O14773-2	8466300	0	
Q92629-3	8383200	3835000	2.19
P61225	8115600	0	
P98160	7959400	0	
P11413	7834100	0	
CON__Q3SZR3	7726200	0	
B5MCT8	7644500	0	
P40429	7278400	0	
Q5T749	7178300	0	
F8VZJ2	7135900	0	
O00299	6912300	0	
Q5JR95	6898800	0	
E9PPR1	6862700	0	
P53680-2	6597400	0	

Protein ID	LFQ nonmin-ECM	LFQ min-ECM	ratio
G3V1K1	6450900	0	
M0R3H0	6443300	0	
Q13618-3	6435500	0	
P06702	6088700	0	
P34810-2	5961200	0	
O43854-2	5804100	0	
P62304	5617500	0	
Q5T8U3	5577300	0	
O00159-2	5550800	0	
E9PJD9	5477200	0	
CON__P41361	5447300	0	
B3KQ59	5426500	0	
A8MT72	5421300	0	
Q5HY57	5406400	0	
P16401	5381100	0	
CON__P06868	5316400	0	
J3KTJ8	5291400	0	
P08240	5200800	0	
O75438	5156100	0	
Q9UBR2	5041500	0	
Q9HCI5	5013600	0	
C9JXB8	4925800	0	
P62070	4895100	0	
Q13509	4864800	0	
CON__Q95121	4854200	0	
Q15904	4826100	0	
O43493-4	4784300	0	
Q5VXJ5	4686300	0	
O75348	4664900	0	
H0Y750	4653800	0	
J3QL05	4578000	0	
K7EM02	4552000	0	
P08754	4483400	0	
P26641	4475300	0	
B4E022	4440200	0	
P20674	4369000	0	
E9PNA6	4245000	0	
E9PB77	4102400	0	
Q9ULC3	3978800	0	
Q6KB66-2	3819000	0	
F8WCJ1	3779800	0	
P17693	3770200	0	
Q5T4L4	3676800	0	
CON__Q0V8M9	3675900	0	

Protein ID	LFQ nonmin-ECM	LFQ min-ECM	ratio
D6RG13	3647900	0	
G3V279	3476200	0	
Q9BXJ4-2	3457500	0	
P35555	3383200	0	
P26373-2	3338000	0	
P62316	3337000	0	
Q9Y3D6	3262500	0	
A8MZH8	3251800	0	
CON__Q2KJ62	3222000	0	
REV__H3BU65	3171900	0	
Q13492-4	3088700	0	
Q5T750	3028000	0	
Q5H9B4	3026500	0	
Q96DA6-2	2971600	0	
J3QS96	2956500	0	
J3QRM9	2938800	0	
Q5T8R3	2907700	0	
Q96RM1	2754500	0	
O43795-2	2731200	0	
Q9Y3U8	2720600	0	
P07093-2	2712400	0	
Q96BM9	2709600	0	
C9J4Z3	2661000	0	
P01031	2647000	0	
H7C5K4	2537000	0	
CON__Q9TT36	2526200	0	
J3KSR8	2489400	0	
Q9NTK5-2	2485100	0	
E7EPB3	2373200	0	
P49207	2370900	0	
Q9BQJ4	2330500	0	
Q9NZL4	2319400	0	
CON__P17697	2225300	0	
P18124	2155600	0	
F8WBS5	2036100	0	
Q9UI95	1976800	0	
CON__P00735	1975700	0	
P56556	1969800	0	
Q6EMK4	1951600	0	
G3V2F7	1925100	0	
G3V1B3	1757400	0	
O95837	1716400	0	
C9JPX5	1626400	0	
Q15063-7	1591600	0	

Protein ID	LFQ nonmin-ECM	LFQ min-ECM	ratio
P53708	1514200	0	
P63208	1391000	0	
H0YKU1	1350200	0	
P18859	1338900	0	
Q12846-2	1183500	0	
O00160	1175300	0	
H0YNE9	1162100	0	
Q04721	1143800	0	
M0R0P7	1096200	0	
P20645	1079400	0	
X6RCE4	1068100	0	
O95139	1062500	0	
B4DIT7	969870	0	
J3KSQ5	946380	0	
H0YEU0	939320	0	
K7ERA3	937910	0	
O60296	934210	0	
O00592-2	931470	0	
P53999	912410	0	
P08729	907080	0	
Q9Y2L8	874990	0	
S4R456	832160	0	
Q6UWF9	825840	0	
O15484	818710	0	
C9JNK6	749000	0	
CON__Q2KIF2	645370	0	
CON__ENSEMBL:ENSBTAP00000032840	365370	0	
P14923	333540	0	
Q8N1N4-2	301060	0	
Q96EU7	267200	0	

Supplementary Table 2. Proteins detected only in the min-ECM and more than 2-fold upregulated in this ECM than in nonmin-ECM. Proteins are indicated as protein IDs and ranked for abundance in min-ECM. Color scale represents difference in abundance between the ECMs.

Protein ID	LFQ min-ECM	LFQ nonmin-ECM	ratio
P15144	2731900000	1218800000	2.24
P08133	2720200000	1272400000	2.14
P08758	2687800000	1096900000	2.45
Q14195	2182700000	0	
REV__S4R403	2141700000	0	
P21333-2	855700000	293020000	2.92
Q09666	834240000	283210000	2.95
Q6UVK1	735210000	345630000	2.13
P10809	686720000	296740000	2.31
P08648	583020000	230510000	2.53
P56199	564630000	54704000	10.32
Q9UBG0	432950000	208340000	2.08
Q08431	415250000	193500000	2.15
P07099	415110000	207480000	2.00
P40939	338310000	161810000	2.09
P40926	326330000	130410000	2.50
P00367	305550000	119680000	2.55
P36269	258740000	0	
Q2Y0W8-5	238890000	0	
O75396	229140000	75247000	3.05
P30048-2	225600000	78019000	2.89
Q9Y490	186520000	35876000	5.20
P31949	158370000	58743000	2.70
P49748-2	146340000	0	
P05186	123980000	57666000	2.15
Q9Y4L1	122400000	22283000	5.49
REV__Q96HY7	120770000	0	
P04040	109890000	32742000	3.36
Q96AY3	106700000	28681000	3.72
Q9NYU2-2	106160000	44420000	2.39
O94925-3	104920000	18518000	5.67
O95202	101470000	0	
O95831-3	101410000	10233000	9.91
P50995-2	100400000	47118000	2.13
P11498	98381000	8408200	11.70
Q99715-4	97952000	26615000	3.68
P51659	95062000	38670000	2.46
Q99798	94651000	0	
P10620	90317000	29657000	3.05
P22307-6	89976000	38073000	2.36
Q02218	86806000	0	

Protein ID	LFQ min-ECM	LFQ nonmin-ECM	ratio
P56134-3	86330000	39474000	2.19
Q6YHK3	86195000	21684000	3.98
P04179-4	85247000	10881000	7.83
P27658	83266000	28679000	2.90
Q9P0L0	79930000	32683000	2.45
Q15165-3	77950000	31286000	2.49
P00167-2	77902000	30302000	2.57
B4DJV2	75996000	6639400	11.45
Q969H8	74151000	30184000	2.46
Q99714	72570000	2986100	24.30
P30084	68741000	0	
P07954-2	68611000	18908000	3.63
Q01628	67864000	21718000	3.12
Q13162	66518000	23452000	2.84
P36957	66164000	29258000	2.26
Q9BSJ8	65878000	24738000	2.66
Q3SY69	64289000	0	
Q86UY0	61952000	20666000	3.00
P11047	58530000	7170900	8.16
Q9UGT4	57581000	0	
P42704	56376000	0	
O95302	56266000	24629000	2.28
Q15149	56087000	0	
P14384	49315000	0	
Q04837	48685000	23890000	2.04
P30040	48143000	21423000	2.25
Q9Y2Q3	47958000	11843000	4.05
K7EJE8	47670000	0	
Q9UJS0	47118000	4468800	10.54
P24752	45815000	0	
P21912	45414000	21879000	2.08
Q8WWI5-3	44611000	0	
REV__H0Y547	41561000	0	
B4DT77	41156000	14336000	2.87
Q9BS26	41127000	12823000	3.21
Q00765	40765000	15152000	2.69
Q8TCT9-5	38600000	16654000	2.32
P07942	38454000	0	
Q7Z3B1	35259000	0	
P49419-2	34825000	10717000	3.25
P54920	33763000	16447000	2.05
Q01082	33669000	2243600	15.01
P05091	32647000	6897900	4.73
E9PEP6	32474000	12774000	2.54

Protein ID	LFQ min-ECM	LFQ nonmin-ECM	ratio
P00505	31535000	0	
F8VQX6	31456000	0	
Q13011	30934000	13271000	2.33
P50213	30326000	0	
O94919	30065000	0	
P43304-2	29011000	5125500	5.66
P50416-2	28485000	0	
O00116	27261000	0	
P16435	26627000	0	
P30519	25985000	0	
Q07021	25825000	0	
Q99805	25304000	0	
Q96I99	25060000	0	
P26885	25048000	10529000	2.38
O14735-3	23956000	6042900	3.96
Q8N0U8	23501000	0	
Q9UIJ7	23465000	0	
Q96HE7	23286000	0	
Q8NB49-2	22969000	0	
P21397	22886000	0	
Q8TCJ2	22098000	0	
Q9UFN0	22045000	8942700	2.47
P48357-5	21653000	0	
Q9Y3E5	21030000	9801300	2.15
P38117	20920000	0	
O75844	20765000	0	
Q5JRX3	20714000	0	
Q96G23	20606000	0	
Q96D15	20574000	0	
Q9UIQ6-3	20382000	1864100	10.93
O94875-9	20326000	0	
P42126-2	19764000	0	
P62736	19412000	0	
P55809	18967000	0	
J3QQY2	18900000	0	
P09110	18799000	0	
A6NLH6	18780000	0	
Q8N6L1	18651000	0	
P40261	18624000	0	
E7EMM4	17643000	0	
Q5RI15	17574000	7235400	2.43
H0YL12	17415000	0	
O75891	17400000	0	
P49914-2	17077000	0	

Protein ID	LFQ min-ECM	LFQ nonmin-ECM	ratio
Q9HCU0	17059000	0	
Q86WV6	16445000	0	
O95292	16293000	0	
O75369-2	16156000	0	
E9PN66	16154000	0	
Q4G0P3	16103000	0	
Q99523	15991000	0	
Q9Y4D7-2	15955000	0	
F8W031	15776000	0	
P42765	15556000	0	
Q9Y2R0	15478000	6907400	2.24
F5H8J3	14436000	0	
P55145	14377000	5866100	2.45
O94826	14125000	0	
P05362	13874000	0	
Q6ZUX7	13796000	0	
Q16740	13781000	0	
P53621	13663000	0	
P17342-2	13375000	0	
O15254-2	13299000	0	
P54886-2	12949000	0	
Q5BJH7-6	12859000	0	
Q8N5M9	12849000	0	
Q14118	12660000	0	
P57088	12631000	0	
Q9NZN4	12624000	0	
Q5R3B4	12421000	0	
Q7Z4H8	12257000	0	
Q8N1B9	12220000	0	
O95479	12068000	0	
P16278-3	11702000	0	
E9PNJ4	11617000	0	
G3V5P8	11530000	0	
F6SBX2	11506000	0	
Q8N5K1	11125000	0	
Q9HAV0	11047000	0	
P48449-2	10923000	0	
Q86YZ3	10818000	0	
Q9BXK5-4	10780000	0	
P00441	10574000	0	
P30038	10468000	0	
P16112-2	9937100	0	
O14828-2	9789300	0	
Q9Y680-3	9755600	0	

Protein ID	LFQ min-ECM	LFQ nonmin-ECM	ratio
C9JEN3	9686300	0	
O75083	9418600	0	
C9JFR7	9385500	0	
P08559-3	9371300	0	
P10599	9278300	0	
M0QZY4	9229700	0	
P11166	9151400	0	
Q9NTJ5	9138700	0	
Q06136	8958000	0	
Q9P0S9	8901000	0	
Q02252-2	8820400	0	
Q8IVL6-2	8793300	0	
Q16134-3	8649100	0	
O15121	8646800	0	
Q3ZCQ8	8612100	0	
P48960-2	8513600	0	
Q08257-3	8414700	0	
Q7KZF4	8385100	0	
O14548	8298200	0	
P57105	8210400	0	
Q86UP2-2	8060800	0	
H7BZ81	8011400	0	
Q9H251-5	8006300	0	
Q9BU23-2	7981100	0	
Q86UY8	7974000	0	
Q9H061	7858900	0	
Q16836	7815800	0	
P03928	7708100	0	
O75746	7687200	0	
Q9Y673-2	7581600	0	
Q96DZ1-3	7344200	0	
Q0ZGT2-4	7322900	0	
Q9HB66	7245800	0	
Q86Y39	7206200	0	
Q9NR31	7189700	0	
Q9BRR6-2	7181400	0	
Q12931-2	7065800	0	
P61006	7016100	0	
P23368	6990500	0	
Q8WY22	6971300	0	
Q9NZ01	6958700	0	
P41159	6957300	0	
Q6ZXV5-2	6913700	0	
Q6YN16	6808400	0	

Protein ID	LFQ min-ECM	LFQ nonmin-ECM	ratio
G3XAN4	6720400	0	
C9JKQ2	6674300	0	
Q9C0E8-2	6660700	0	
Q9BQE5	6576700	0	
P62834	6566400	0	
F8WBE2	6512700	0	
Q8NBJ7	6422900	0	
E7EPM6	6245900	0	
O15439-2	6241400	0	
H3BSC1	6192000	0	
Q15293	6079000	0	
P53597	6026500	0	
E5RIP4	5875400	0	
Q6UXV4	5868200	0	
REV__Q5JVD3	5728100	0	
O15269	5715900	0	
H3BR27	5712600	0	
Q13636	5628700	0	
O60613	5611800	0	
Q9H0R3-2	5534700	0	
Q9H2U2-6	5531400	0	
Q13641	5445600	0	
Q4KMQ2-3	5441400	0	
Q92544	5434500	0	
J3QRU4	5420900	0	
E5RK01	5325400	0	
Q9UP95-3	5318400	0	
P49821-2	5242700	0	
Q9BUB7-2	5219200	0	
Q99643-5	5181500	0	
Q9H330-2	5100700	0	
Q5T123	5066700	0	
Q9NX40	5021500	0	
Q9Y696	4916100	0	
O75955	4896500	0	
CON__P07224	4780100	0	
P28066	4755600	0	
P10619-2	4719900	0	
K7ENI6	4695400	0	
REV__Q86VH2-3	4609900	0	
H7BXI1	4575500	0	
O00161-2	4530900	0	
Q14696	4512800	0	
Q9HAV7	4463100	0	

Protein ID	LFQ min-ECM	LFQ nonmin-ECM	ratio
P27701-2	4177400	0	
Q6P587	4158800	0	
B4DLH2	4016200	0	
Q15738	3931000	0	
H7C2G3	3868500	0	
Q9HD20-2	3823800	0	
J3QL56	3718600	0	
Q6PI78	3713500	0	
Q13505-3	3627500	0	
Q15155	3625800	0	
Q8NBJ5	3509300	0	
H0YDT8	3502000	0	
Q96CS3	3428400	0	
O43181	3416400	0	
Q92633	3359000	0	
REV__CON__P02672	3299100	0	
Q9BWH2	3268600	0	
P51809-3	3242300	0	
REV__M0R0Q7	3204700	0	
Q5XKP0	3113500	0	
O95573	3056700	0	
Q6IAK0	2986900	0	
F8WAS3	2924500	0	
O14656	2885800	0	
P03897	2867200	0	
O96011-2	2835500	0	
O95571	2821200	0	
Q9Y5J7	2804800	0	
Q9Y305-3	2797900	0	
H7BZI1	2767100	0	
Q7Z7M9	2749100	0	
P81605	2745100	0	
Q5JX45	2685900	0	
Q9Y584	2672300	0	
REV__H7C388	2589800	0	
Q9H0U3	2569500	0	
C9JGJ9	2506200	0	
P84095	2483300	0	
B4DQ51	2477000	0	
B4DN67	2419500	0	
E9PCB6	2360500	0	
Q9BW60	2319700	0	
C9JL85	2243300	0	
Q9H3H5-3	2128500	0	

Protein ID	LFQ min-ECM	LFQ nonmin-ECM	ratio
D6RBS5	2085000	0	
Q969M3	2033200	0	
S4R3U9	1997700	0	
F8VQW8	1971000	0	
H0Y8Z9	1968300	0	
S4R329	1949800	0	
G3V5T4	1945800	0	
A8MT40	1884900	0	
Q14739	1765900	0	
Q5T7F5	1696100	0	
P01034	1694200	0	
P23786	1668200	0	
Q9Y320-2	1584300	0	
Q9BRK3-3	1578300	0	
Q9HBH5	1549900	0	
O14521-2	1548900	0	
P28838-2	1544400	0	
F5H261	1489700	0	
H0YLB6	1467000	0	
O15438	1397200	0	
Q96QK1	1378900	0	
H0YHJ8	1368200	0	
Q9UM54-5	1353500	0	
P06748-2	1338400	0	
REV__Q5T4B2-2	1294900	0	
F5H5N1	1294400	0	
Q9UGQ3-2	1262200	0	
Q6UWP7-3	1252400	0	
P08842	1214400	0	
Q8WVX3	1185500	0	
Q9P0J1	1185500	0	
F8WAX7	1178700	0	
I3L1T3	1145400	0	
Q8NFQ8	1129500	0	
H0YC95	1110600	0	
Q6TDP4	1105600	0	
E9PP42	1079000	0	
C0H5Y7	1041700	0	
O94911	1034600	0	
U3KQU4	1007600	0	
F5H459	970120	0	
B5MCE2	920620	0	
P08473	910030	0	
C9JY28	903360	0	

Protein ID	LFQ min-ECM	LFQ nonmin-ECM	ratio
K7EP56	890940	0	
P52815	859090	0	
Q9NZ08	854950	0	
H7BXK9	829150	0	
M0R1E0	822350	0	
P00156	806720	0	
H7C613	787170	0	
Q5T3Q7	780680	0	
H7BXL1	768380	0	
F5H4N4	662750	0	
E9PSI1	642460	0	
D6RF69	490670	0	
O75051	464780	0	
P05771	461470	0	
H7BYE5	456700	0	
H0YNE5	332980	0	
Q7KYR7-6	284500	0	

Supplementary Table 3. List of proteins belonging to the indicated GO terms of the GO analysis of the 290 proteins upregulated in nonmin-ECM and the 366 proteins upregulated in min-ECM. Proteins are indicated as Gene names.

GO term	nonmin-ECM			min-ECM		
	Fold enrichment	# proteins	Gene names	Fold enrichment	# proteins	Gene names
GO:0006414 translational elongation	**22.96**	42	RPL17, RPL14, RPL13, RPL27A, RPS15A, RPL36, RPS3, RPS25, RPL30, RPS27, RPL7, RPL31, RPS3A, RPL9, RPL34, RPLP1, RPL7A, RPL10A, RPS24, RPL35A, RPL26, RPL27, RPS9, RPL23A, RPL24, RPS4X, RPS8, RPS7, RPS18, RPS19, RPL23, RPL18A, RPS16, RPL13A, RPL22, RPS14, RPL21, RPS15, RPS13, EEF1G, RPL37A, EEF1D	0.00		
GO:0030162 regulation of proteolysis	**9.38**	9	HSP90AB1, A2M, SERPINE2, APOE, SERPINA5, RAB23, IGF2, TIMP3, TIMP1	0.00		
GO:0007160 cell-matrix adhesion	**6.82**	11	CD44, CTGF, ITGA8, AGT, ITGB6, ITGA7, ITGA11, ITGA2, VTN, THY1, FN1	0.00		
GO:0000786 nucleosome	**6.20**	8	H2AFV, HIST1H1C, HIST1H4A, HIST1H2BL, HIST1H1B, H3F3B, HIST1H2AJ, HIST3H2BB	0.00		
GO:0031012 extracellular matrix	**2.97**	21	HAPLN1, TF, STX4, EFEMP2, TNC, FBN1, HSPG2, CCDC80, VTN, POSTN, TIMP3, TIMP1, AHSG, EMILIN1, GPC4, CD44, CTGF, GPC6, TGFBI, ADAMTS1, FN1	0.91	8	CD248, ACAN, DAG1, COL12A1, LAMC1, LAMB1, SOD1, COL8A1

GO term	nonmin-ECM			min-ECM		
	Fold enrichment	# proteins	Gene names	Fold enrichment	# proteins	Gene names
GO:0005739 mitochondrion mitochondrion	0.90	20	NDUFB11, NDUFA3, NDUFB6, NDUFA8, PHB, NDUFA6, MTX2, CLU, CHCHD3, DPYSL2, COX5A, NDUFB1, FIS1, PTRF, C1QTNF3, TPP1, TGM2, CTSB, DNAJC19, ATP5J	**4.10**	114	PDP1, GRPEL1, IARS2, OGDH, GOT2, FAHD1, BAK1, AGPS, TIMM9, PDHA1, HADH, TMEM14C, ACAA2, PDPR, ALDH6A1, SUCLG2, SUCLG1, LYRM4, TMEM126A, SYNJ2BP, BCL2L13, LETM1, CLPP, LRPPRC, MDH2, HSD17B10, ACADSB, ME2, GLUD1, MTX1, CTSA, PTRH2, ACAT1, HADHA, GSTK1, ALDH4A1, FH, GPD2, ATP5J2, MAOA, AK3, C21ORF33, AFG3L2, ABCB6, PPA2, IDH3A, SLC25A12, SLC25A13, TOMM70A, NDUFV1, GLS, ALDH2, HSPD1, PC, CPT2, PRDX4, TIMM50, PRDX3, ACOT9, NDUFS7, TMEM173, LONP1, NDUFS4, CAT, ACAD9, DHTKD1, FUNDC2, ACO2, SSBP1, AIFM1, CYCS, TMEM70, CYB5A, NDUFA10, NDUFA11, TIMM22, LAP3, ACADVL, TRAP1, ALDH7A1, C1QBP, CLIC4, TXN, NDUFB3, APOOL, ALDH18A1, ECH1, ETHE1, ECHS1, COX7A2L, ACSL1, MRPL12, OXCT1, PITRM1, ETFDH, HSD17B4, ACSL3, ETFB, SCO1, ETFA, DLST, NDUFA5, CS, SOD1, CPT1A, SOD2, SDHB, PEX11B, HSDL2, SDHC, SDHD, NLN, SCP2, MGST1
GO:0016192 vesicle-mediated transport	0.86	9	STX4, GNAI3, PICALM, APOE, AP2S1, TRAPPC5, MYO1F, M6PR, AHSG	**2.12**	25	COPA, CNIH, AP3S1, NAPA, BCAP29, SEC22B, VPS35, SNAP23, SAR1A, EHD2, ELMOD2, RAB8A, SCAMP3, MYO6, RAB4B, MRC2, MFGE8, ERGIC2, FLNA, VAMP7, TXNDC5, CPNE1, SORT1, YIPF5, VAMP2
GO:0005509 calcium ion binding	1.71	29	MYL6, MYL1, S100A9, PRSS1, ITGA11, CRNN, EDIL3, TKTL1, MYL9, MACF1, GALNTL5, PRSS3, TGM2, CACNA2D1, CAPNS1, EFEMP2, FBN1, ITGA2, TKT, MYL12A, CAPN2, S100A13, PLG, NOTCH2, CDH13, FLG, ITGA8, ITGA7, F2	**1.87**	34	PDP1, COPA, FKBP9, HRNR, FKBP7, GALNT5, CD248, DAG1, ANXA6, FAHD1, CD97, ANXA7, ANO6, EHD2, CDH23, GPD2, STS, MRC2, S100A11, ITGA1, STIM1, ANXA5, PRKCB, SLC25A12, NUCB1, LETM1, SLC25A13, ITGA5, ANXA11, SUMF2, FKBP10, RCN3, PROS1, RCN1

Supplementary Table 4. List of proteins detected only in activin-ECM and more than 2-fold up-regulated in activin-ECM compared to min-ECM. Proteins are indicated as Protein IDs and ranked for abundance in the activin-ECM. Color scale represents difference in abundance between the ECMs.

Protein ID	LFQ activin-ECM	LFQ min-ECM	ratio
REV__K4DI97	27524000000	0	
CON__P02769	16428000000	6914000000	2.38
G3V5X4	4611100000	0	
REV__Q9Y4K1	1631000000	0	
Q9H1P3-2	1474200000	0	
B7ZBT8	1361000000	0	
CON__Q0IIK2	1161000000	385210000	3.01
R4GNC5	324110000	0	
Q99715-4	284070000	97952000	2.90
Q96M53-2	222780000	0	
P62805	185390000	89920000	2.06
Q9UKX5	151930000	71091000	2.14
P08779	133710000	42336000	3.16
CON__Q3MHN5	129110000	29429000	4.39
CON__Q9TRI1	108120000	44790000	2.41
CON__Q58D62	92398000	35301000	2.62
P02538	89464000	36998000	2.42
CON__Q3SZ57	85110000	38815000	2.19
REV__I3L4H9	78493000	0	
REV__H0YLX2	71133000	0	
CON__Q3T052	65206000	4428600	14.72
P02533	55961000	27303000	2.05
CON__ ENSEMBL: ENSBTAP00000007350	53061000	17417000	3.05
P05121	47978000	0	
CON__Q9N2I2	39370000	0	
Q9Y6C2	31017000	12268000	2.53
M0QZ66	29269000	0	
P05090	29250000	0	
CON__Q2UVX4	29037000	0	
CON__Q3SZH5	28079000	0	
P62081	24896000	12143000	2.05
Q4V9L6	24534000	0	
Q3SY84	18064000	0	
P59666	15778000	0	
CON__Q3Y5Z3	15465000	6059800	2.55
Q04695	14618000	0	
O95803-2	14486000	0	
G3V576	14038000	0	
C9J719	13456000	0	

Protein ID	LFQ activin-ECM	LFQ min-ECM	ratio
P62277	12213000	0	
Q15388	10181000	0	
Q15393	9808800	0	
P04156-2	9689700	0	
CON__Q3SZR3	9361400	0	
Q0VGL1	8892400	0	
S4R3I5	8811500	0	
E5RGY0	8787500	0	
Q96PV0-3	8643700	0	
P62263	8274200	0	
Q3ZAQ7	8226300	0	
B4DKJ3	8224900	0	
Q16647	8205000	0	
CON__P00978	8050200	0	
F5H2J3	7822600	0	
Q9UHQ9	7664200	0	
Q8N257	7533500	0	
D6RCD0	7511000	0	
G5E9Z2	6732900	0	
B4DFL2	6633100	0	
Q6RW13	6594900	0	
Q16658	6265100	0	
O43674-2	6242900	0	
E9PG39	6044000	0	
F5GWH5	5811400	0	
Q9NPJ3-2	5731600	0	
P53680-2	5505900	0	
O95182	5499000	0	
P98160	5461300	0	
P26440-2	5409700	0	
P01877	5338300	0	
P26232-3	5265500	0	
P17152	5180600	0	
P11413	5142400	0	
Q5D862	5048000	0	
P20674	4995900	0	
G3V2G6	4937000	0	
Q9UGP8	4904100	0	
O15145	4813600	0	
CON__P28800	4812500	0	
Q16850-2	4801600	0	
P29279	4789600	0	
Q9H7Z7	4776400	0	
CON__Q0VCM5	4743700	0	

Protein ID	LFQ activin-ECM	LFQ min-ECM	ratio
Q969E2-2	4477100	0	
Q9Y3Q3	4446100	0	
REV__Q9NP60	4443800	0	
Q15067-2	4428100	0	
P06702	4419500	0	
P63096	4363000	0	
I3L4G8	4152300	0	
CON__P41361	4142800	0	
H7BXT7	4101500	0	
P48668	4091800	0	
O00461	4048700	0	
Q9H1C7	4003700	0	
Q16822-2	3950500	0	
Q5JWB9	3933000	0	
O43837-2	3925100	0	
A6NGW1	3924600	0	
Q15582	3922100	0	
Q9NX76	3911600	0	
O75348	3853100	0	
E9PKG6	3820200	0	
Q9BVK8-2	3743500	0	
Q86UQ4	3720600	0	
P15924	3530600	0	
Q9BX68	3441400	0	
REV__Q6ZT07	3403900	0	
Q8N5G0-2	3385900	0	
P32455	3341700	0	
P62745	3322900	0	
J3KTF4	3229300	0	
Q96HY6-2	3172400	0	
Q5T749	3120300	0	
P26641	3063200	0	
Q9NW15	3018000	0	
P04259	2995800	0	
I3L161	2954800	0	
Q9UBR2	2913600	0	
CON__A2I7N1	2911500	0	
Q5T8R3	2875500	0	
O43731	2868900	0	
O75477	2856600	0	
H0YJL5	2797600	0	
CON__Q28085	2789200	0	
Q9BV81	2766000	0	
H0YB38	2749000	0	

Protein ID	LFQ activin-ECM	LFQ min-ECM	ratio
H3BUU9	2723700	0	
M0R1B0	2696400	0	
Q5BJD5-3	2683100	0	
Q15800-2	2526500	0	
P60602-2	2478000	0	
P00395	2467600	0	
Q7Z3Y8	2463700	0	
P14174	2422600	0	
J3KRS1	2315800	0	
K7EIN4	2296900	0	
H0YLY7	2284500	0	
H0Y8N7	2247800	0	
O75521-2	2233300	0	
Q68D91-2	2069800	0	
P62316	2068300	0	
P02788-2	2058900	0	
F5GXC8	2028300	0	
Q5W111-2	1977700	0	
B4DWZ5	1957700	0	
O14957	1956700	0	
Q9P032	1870500	0	
B1AK81	1831000	0	
Q9H2V7-3	1826600	0	
Q14344-2	1769800	0	
P78536-2	1657700	0	
O94874-2	1621700	0	
C9J0K6	1593400	0	
Q96N66-3	1587500	0	
P31151	1503900	0	
H0YKI0	1497100	0	
P21281	1496500	0	
REV__A4FU49-5	1436100	0	
K7ELD9	1430900	0	
CON__A2I7N3	1402700	0	
P98095	1382500	0	
O75643	1349600	0	
P30533	1306300	0	
Q9UGM3-9	1302500	0	
B7Z3F5	1283800	0	
E9PE82	1239800	0	
G3V0F2	1229900	0	
REV__C9J4B8	1175400	0	
E9PN41	1162400	0	
C9K068	1162300	0	

Protein ID	LFQ activin-ECM	LFQ min-ECM	ratio
K7EJM8	1093100	0	
P08311	1044100	0	
H0YK87	1040300	0	
M0R026	1013400	0	
H0YAX3	1012900	0	
O95297-4	999190	0	
P17568	983410	0	
H7C533	952260	0	
F5H3C1	948740	0	
CON__Q05B55	923200	0	
K7EPU3	902950	0	
Q96EL3	870710	0	
Q9H0X4	863050	0	
CON__P02662	844310	0	
Q9BU61	831300	0	
P82909	830680	0	
Q8WUH6	794960	0	
CON__P02666	794650	0	
Q16706	792150	0	
H0YDP7	758620	0	
H0Y430	755410	0	
H7C0V0	739180	0	
C9JCH4	734340	0	
O15357-2	710220	0	
P20908	704110	0	
Q5VT94	701570	0	
P14923	656640	0	
P05164-2	654240	0	
P15289-2	648670	0	
Q8IY95-2	638210	0	
P15529-15	624670	0	
Q9Y3L5	599150	0	
Q9H6X2-3	571480	0	
Q02413	535600	0	
Q13835-2	456190	0	
F8VV32	443880	0	
H0YD98	255420	0	
O95470	144760	0	
Q96Q11-2	111900	0	

Supplementary Table 5. Proteins detected only in min-ECM and at more than 2-fold upregulated in this ECM than activin-ECM. Proteins are indicated as Protein IDs and ranked for abundance in min-ECM. Color scale represents difference in abundance between the ECMs.

Protein ID	LFQ min-ECM	LFQ activin-ECM	ratio
Q14195	2182700000	0	
REV__S4R403	2141700000	0	
Q9UBG0	432950000	188880000	2.29
Q2Y0W8-5	238890000	0	
P05186	123980000	49732000	2.49
REV__Q96HY7	120770000	0	
Q96AY3	106700000	36980000	2.89
O95831-3	101410000	35408000	2.86
P26038	64976000	28032000	2.32
P11047	58530000	26768000	2.19
Q9UGT4	57581000	24673000	2.33
Q01082	33669000	9239800	3.64
E9PEP6	32474000	13946000	2.33
P43304-2	29011000	4543200	6.39
K7EMV3	23100000	0	
P21397	22886000	8926200	2.56
Q9UIQ6-3	20382000	9770000	2.09
A6NLH6	18780000	0	
Q8N6L1	18651000	0	
P06744	17477000	0	
P49914-2	17077000	0	
Q4G0P3	16103000	0	
Q6ZUX7	13796000	0	
Q8N5M9	12849000	0	
Q8N1B9	12220000	0	
O95479	12068000	0	
P43007	11869000	0	
G3V5P8	11530000	0	
P62750	11341000	0	
E9PP23	10962000	0	
Q86YZ3	10818000	0	
Q9BXK5-4	10780000	0	
P00441	10574000	0	
Q16555	10328000	0	
O14828-2	9789300	0	
P36871	9692800	0	
C9JEN3	9686300	0	
P47755	9641500	0	
O75083	9418600	0	
P10599	9278300	0	
M0QZY4	9229700	0	
Q06136	8958000	0	
Q8IVL6-2	8793300	0	

Protein ID	LFQ min-ECM	LFQ activin-ECM	ratio
Q16134-3	8649100	0	
O14548	8298200	0	
P57105	8210400	0	
Q9H251-5	8006300	0	
P03928	7708100	0	
O43678	7445600	0	
Q9HB66	7245800	0	
Q86Y39	7206200	0	
Q9BRR6-2	7181400	0	
Q12931-2	7065800	0	
P61006	7016100	0	
P23368	6990500	0	
P41159	6957300	0	
Q6YN16	6808400	0	
H3BSC1	6192000	0	
Q15293	6079000	0	
P53597	6026500	0	
E5RIP4	5875400	0	
Q6UXV4	5868200	0	
Q7Z5G4	5751000	0	
REV__Q5JVD3	5728100	0	
H3BR27	5712600	0	
Q9H0R3-2	5534700	0	
Q9H2U2-6	5531400	0	
Q13641	5445600	0	
Q4KMQ2-3	5441400	0	
Q92544	5434500	0	
J3QRU4	5420900	0	
E5RK01	5325400	0	
Q9BUB7-2	5219200	0	
O14579	5107000	0	
Q9H330-2	5100700	0	
Q5T123	5066700	0	
Q9Y696	4916100	0	
O75955	4896500	0	
CON__P07224	4780100	0	
P28066	4755600	0	
K7ENI6	4695400	0	
REV__Q86VH2-3	4609900	0	
O00161-2	4530900	0	
P02656	4337600	0	
P50395	4232800	1787900	2.37
Q6P587	4158800	0	
O60701	4063800	0	
B4DLH2	4016200	0	
P23229-4	3865000	0	

Protein ID	LFQ min-ECM	LFQ activin-ECM	ratio
J3QL56	3718600	0	
O43504	3669400	0	
Q15155	3625800	0	
Q8NBJ5	3509300	0	
Q96CS3	3428400	0	
Q92633	3359000	0	
REV__CON__P02672	3299100	0	
REV__M0R0Q7	3204700	0	
Q5XKP0	3113500	0	
O95573	3056700	0	
Q6IAK0	2986900	0	
F8WAS3	2924500	0	
P03897	2867200	0	
O96011-2	2835500	0	
O95571	2821200	0	
Q9Y5J7	2804800	0	
Q9Y305-3	2797900	0	
Q7Z7M9	2749100	623500	4.41
P81605	2745100	0	
Q5JX45	2685900	0	
Q9Y584	2672300	0	
REV__H7C388	2589800	0	
C9JGJ9	2506200	0	
P84095	2483300	0	
B4DQ51	2477000	0	
B4DN67	2419500	0	
E9PCB6	2360500	0	
Q9BW60	2319700	0	
C9JL85	2243300	0	
Q9H3H5-3	2128500	0	
D6RBS5	2085000	0	
Q969M3	2033200	0	
S4R3U9	1997700	0	
P02461-2	1985700	0	
F8VQW8	1971000	0	
H0Y8Z9	1968300	0	
S4R329	1949800	0	
G3V5T4	1945800	0	
A8MT40	1884900	0	
Q14739	1765900	0	
Q5T7F5	1696100	0	
P01034	1694200	0	
P23786	1668200	0	
Q9Y320-2	1584300	0	
Q9BRK3-3	1578300	0	
Q9HBH5	1549900	0	

Protein ID	LFQ min-ECM	LFQ activin-ECM	ratio
O14521-2	1548900	0	
F5H261	1489700	0	
H0YLB6	1467000	0	
O15438	1397200	0	
Q96QK1	1378900	0	
H0YHJ8	1368200	0	
Q9UM54-5	1353500	0	
REV__Q5T4B2-2	1294900	0	
F5H5N1	1294400	0	
Q9UGQ3-2	1262200	0	
Q6UWP7-3	1252400	0	
P08842	1214400	0	
Q8WVX3	1185500	0	
Q9P0J1	1185500	0	
F8WAX7	1178700	0	
I3L1T3	1145400	0	
Q8NFQ8	1129500	0	
H0YC95	1110600	0	
Q6TDP4	1105600	0	
E9PP42	1079000	0	
C0H5Y7	1041700	0	
O94911	1034600	0	
U3KQU4	1007600	0	
F5H459	970120	0	
B5MCE2	920620	0	
P08473	910030	0	
C9JY28	903360	0	
K7EP56	890940	0	
P52815	859090	0	
Q9NZ08	854950	0	
H7BXK9	829150	0	
M0R1E0	822350	0	
P00156	806720	0	
H7C613	787170	0	
Q5T3Q7	780680	0	
H7BXL1	768380	0	
F5H4N4	662750	0	
E9PSI1	642460	0	
D6RF69	490670	0	
O75051	464780	0	
P05771	461470	0	
H7BYE5	456700	0	
H0YNE5	332980	0	
Q7KYR7-6	284500	0	

Supplementary Table 6. List of proteins belonging to the indicated GO terms of the GO analysis of the 210 proteins upregulated in activin-ECM and the resulting 165 proteins upregulated in min-ECM. Proteins are indicated as Gene names.

GO term	activin-ECM			min-ECM		
	Fold Enrichment	# proteins	Gene names	Fold Enrichment	# proteins	Gene names
GO:0030414 peptidase inhibitor activity	**6.88**	12	AMBP, C4A, C3, ITIH1, SERPINF2, FETUB, SERPINA5, AGT, SERPINE1, ITIH4, SERPINC1, ITIH2	0.00		
GO:0005198 structural molecule activity	**3.74**	27	MRPS36, KRT6C, MPZL1, KRT6A, KRT6B, FLG2, MRPL13, KRT27, ARPC3, COMP, COL12A1, MRPL1, COL5A1, EMILIN1, CTNNA2, RPS7, JUP, PKP1, KRT17, KRT16, FBLN2, RPS14, KRT14, MRPL49, DSP, RPS13, KRT71	0.00		
GO:0005739 mitochondrion	**2.29**	35	NDUFAF4, MRPS36, ACOX1, NDUFB5, PTGES2, NDUFB7, HINT2, ROMO1, COX5A, NDUFAF3, SLC25A20, MRPL13, UQCR11, IVD, GBAS, IDH2, ACOT13, SUCLA2, AGK, MRPL53, MRPL1, NDUFA3, FECH, ACADS, NDUFA7, FDXR, IDH3B, PCK2, TRNT1, C2ORF47, MRPL49, TOMM20, DSP, SPNS1, DUT	**3.34**	44	PDP1, APOOL, ACADSB, ME2, CPT2, ETHE1, COX7A2L, ACOT9, FAHD1, NDUFS7, BAK1, MRPL12, TIMM9, ETFDH, ACAD9, DHTKD1, ACSL3, SCO1, GPD2, PDPR, NDUFA5, NDUFA2, AIFM1, MAOA, SUCLG1, LYRM4, TMEM70, SYNJ2BP, DPYSL2, NDUFA10, AFG3L2, BCL2L13, SOD1, ABCB6, PPA2, NDUFA11, TIMM22, TRAP1, PEX11B, HSDL2, CLIC4, SDHD, TXN, NLN
GO:0044421 extracellular region part	**2.15**	29	GC, TF, C3, MIF, APOD, ALB, CTGF, COMP, AGT, TGFBI, CFH, SERPINC1, COL12A1, C4A, LYZ, HSPG2, PCDH15, ADIPOQ, COL5A1, EMILIN1, AFP, ORM1, FBLN2, SERPINF2, NUCB2, DEFA3, ARSA, MPO, CMTM6	0.77	9	LEP, GPI, FGA, APOC3, COL3A1, CST3, KDSR, LAMC1, SOD1
GO:0031090 organelle membrane	**1.94**	30	NDUFAF4, ACOX1, NDUFB5, DERL1, NDUFB7, CYP51A1, CHMP6, AP2S1, ATP6V1G1, COX5A, NDUFAF3, SLC25A20, PIGK, UQCR11, VMA21, RHOB, AGK, SGPL1, NDUFA3, FECH, NDUFA7, FDXR, VTI1B, ERLIN1, MAN2A1, SYNE2, NUCB2, TOMM20, SPNS1, DMBT1	**2.93**	39	APOOL, DERL2, CPT2, CNIH, ATL1, COX7A2L, NDUFS7, FAHD1, BAK1, FMO3, TIMM9, ETFDH, ACSL3, LBR, SCO1, GPD2, NDUFA5, SCAMP3, STS, NDUFA2, MYO6, MAOA, SUCLG1, TMEM70, DPAGT1, SYNJ2BP, NDUFA10, KRTCAP2, AFG3L2, ABCB6, NDUFA11, TIMM22, MGAT1, PEX11B, SDHD, KDSR, VAMP2, NOMO1, COPE

Supplementary Table 7. List of the 538 proteins shared by the 3 devitalized ECMs. Proteins are indicated as Protein IDs and Gene ID-alphabetically ordered.

CON__Q2KJF1	P24539	B4DZI8	P07954-2	P08107
CON__ENSEMBL:ENS-BTAP00000024146	O75947	Q5RI15	Q96AY3	P11021
	P56385	P13073	Q9NYL4-2	P11142
I3L4X2	P56134-3	P10606	P26885	P38646
P68032	E9PN17	P14854	O95302	P04792
P63261	P48047	P09669	P21333-2	P10809
P12814	P61421	P14406	Q14254	P61604
O43707	P61769	C9JP16	P02751-17	Q92743
P61160	O75531	E9PR44	Q10472	Q9Y4L1
P61158	P51572	B4DJV2	G3V1S6	Q9Y5U9
CON__Q3Y5Z3	P35613-2	Q6UVK1	Q14697	Q01628
CON__Q3SZ57	Q969H8	Q96CG8-3	P04406	P11717
Q09666	CON__ENSEMBL:ENS-BTAP00000007350	G3XAM7	P41250	Q70UQ0-4
CON__P12763		B4DGU4	P04062-4	P46940
O95831-3	P54289-4	P07858	CON__Q3MHN5	P56199
CON__P02769	Q05682-5	P07339	P50395	Q9UKX5
Q13740-2	P27797	P00167-2	Q92896	P26006
P30837	O43852	J3KNF8	Q9H4G4	P08648
P05091	P27824	P00387-2	O94925-3	Q13683-9
J3QRD1	Q01518-2	Q53TN4-3	P00367	P06756-3
P49419-2	P04632	P08574	P29992	P05556
P04075	P52907	F5GXX5	P04899	P18084
P05186	P47756-2	P39656	P50148	CON__Q9TRI1
P15144	P04040	B7Z6B8	P63092-3	CON__Q3T052
P04083	Q03135	Q9Y394-2	P62873	P24390
P50995-2	P51636-2	P09622	P62879	CON__P01044-1
P07355	Q96A33-2	P36957	Q9UBI6	P04264
P09525	Q6YHK3	Q9UBS4	F5H6U7	P13645
P08758	E9PMR4	Q9H3Z4-2	P35052	P02533
P08133	Q5ZPR3-3	O60762	O75487	P08779
B4DT77	H0YD13	P60981	P43304-2	P35908
Q9HDC9	Q08722-2	E7EQU2	E7ETY7	P13647
CON__P15497	E9PNW4	B4DKB2	P06396-2	P02538
CON__Q03247	F8VNT9	Q13011	Q9Y2Q3	P35527
CON__P17690	E9PJK1	Q5VTE0	P09211	P11047
G3V1B6	A6NNI4	P13639	P40939	P11279
P84077	P14209	Q14240	P55084-2	B4E2S7
P18085	P60953	P38919	CON__P01966	H0YFI1
J3KTF8	P55290	Q8N766-3	CON__Q3SX09	Q9Y2Q5
O75915	A8MWK3	Q15006	P31937	Q9UHA4-2
Q9NVJ2	O14735-3	Q9Y6C2	Q99878	P00338
O15144	P23528	P17813-2	Q99880	Q32P28
P59998	Q9NZ45	P06733	P62805	P09382
O15511	Q07065	P07099	P30447	P49257
Q12797-10	CON__Q2KIS7	Q969X5-2	P30483	Q12907
Q6DD88	Q00610-2	E5RHW4	P10321	P02545-2
P05023-4	Q9Y2R0	P30040	Q8TCT9-5	Q9UIQ6-3
P54709	Q99715-4	Q9BS26	CON__Q3SZV7	Q07954
P16615-5	P02452	Q9BSJ8	P01112	Q96AG4
P20020-5	P08123	F8W7Q4	Q99714	P61326
P23634-7	P12109	Q92520	Q53GQ0	P55145
P25705	P12110-3	Q12884	P51659	P43121
P06576	P12111-2	CON__ENSEMBL:ENS-BTAP00000016046	P07900	Q8NE86-3
B4DL14	P27658		P08238	P40926
P30049	P21964-2	CON__Q58D62	P14625	Q08431

P10620
O14880
Q14165
Q8N4V1
P50281
Q13724-2
J3QS48
Q9UBG0
P26038
E9PIE4
P00403
Q86UE4
Q14764
P84157-2
Q96S97
P35579
P19105
F8W1R7
P24844
Q9NZM1-6
P54920
Q6PIU2
Q969V3-2
E7ENA9
Q9UI09
B4DEZ3
O00483
P51970
F5H0J3
O96000
O95168-2
O95169-3
E9PH64
O95298
P28331-4
O75306-2
O75489
O43920
E9PN51
P19404
P55769
Q9UFN0
P22392-2
Q13423
Q5JPE7-2
O15118
Q9Y639-1
E9PEP6
P21589
P04181
F6WST4
Q9NRP0
P13674
O15460-2

P07237
Q9Y3D7
P11498
Q9UHG3
P09619
P11177-2
G5EA52
P13667
Q15084-3
CON__P02777
P07737
P18669
P00558
O00264
O15173
P35232
Q99623
P14618
Q02809
O00469
O60568
Q04941
O15031
Q15165-3
O14494
O14495
P62937
P23284
O60831
Q06830
P30048-2
Q13162
P30044-2
Q969G5
P14314-2
P07602
Q9P035
Q6NZI2
Q9Y3E5
P26022
Q8N2H3
P61026
B4DMK0
P61106
Q9NP72
P62820
Q9H0U4
Q9UL25
P61019
B4DJA5
P61020
P51148
P20340-2
P51149

M0R3D4
P63000
P11233
P11234
P61224
O95980
Q00765
Q5T092
Q14699
P61586
P62906
P62913-2
P30050
K7ERI7
E5RI99
P63173
P32969
P05388
P05387
P04843
P04844
P46783
H3BN98
P0CW22
P62269
P39019
P60866
P62851
P23396
M0QZN2
P62081
P10301
Q9P2E9
Q15404-2
O95197-3
Q9NQC3-2
P60903
P31949
R4GN98
P05109
Q14108
Q8NBX0
P22307-6
E7ESK6
Q99470
P31040
P21912
H0YNG3
O75396
P61619
P60468
P60059
Q9UBV2
CON__P34955

CON__Q9TTE1
P50454
Q9H9B4
Q9BWM7
Q92629-3
P34897-3
Q99720
O15427
Q15758
P53007
I3L1P8
Q9UJS0
Q6NUK1
Q00325-2
P12235
P05141
P12236
P08195-2
Q8IWA5-3
Q01650
H0YJ40
P04179-4
P09486
Q9Y6A9
Q15005
P61009
Q13813-3
Q01082
Q9Y6N5
Q9Y5M8
Q04837
C9J3L8
C9JA28
P51571
B4E2V5
Q9UJZ1-2
P46977
Q86Y82
O15400-2
O15260-2
Q16563-2
Q01995
X6RJP6
CON__Q0IIK2
P02786
P07996
E9PIM6
Q9Y490
Q9HD45
P49755
Q15363
Q7Z7H5-3
Q9Y3A6
Q9Y3B3-2

Q9BVK6
Q9BVC6
Q9HC07
Q8TBQ9
Q9BTV4
Q9H3N1
Q96JJ7
Q9H1E5
P24821-4
Q9NS69
Q5JTV8
O43399-2
P60174-1
P09493-3
P07951-2
J3KN67
P67936
B1AH87
Q71U36-2
Q5JP53
Q86UY0
P22314
J3QS39
Q9NYU2-2
Q9UDW1
P14927
P31930
P22695
P47985
O14949
Q96IX5
Q15836
O95183
Q9P0L0
Q99536
P13611-2
P18206-2
P55072
P21796
P45880
Q9Y277
P08670
Q9BQB6-3
CON__Q3ZBS7
P31946-2
P62258
P61981
Q04917
P27348
P63104

Supplementary Table 8. List of proteins belonging to the indicated GO terms of the GO analysis of the 538 proteins shared by the 3 devitalized ECMs.

GO term	fold enrichment	# proteins	Gene names
GO:0016209 antioxidant activity	**6.97**	11	MGST3, ALB, APOE, GSTK1, PRDX4, PRDX5, GPX8, PRDX3, CAT, PRDX1, SOD2
GO:0005200 structural constituent of cytoskeleton	**6.84**	17	KRT6A, TLN1, VIM, ARPC5, TPM1, KRT9, ACTG1, TUBB, KRT5, ARPC2, KRT16, KRT14, KRT1, SPTBN1, KRT2, MSN, SPTAN1
GO:0006414 translational elongation	**5.98**	21	RPLP2, RPS15A, EEF2, RPL38, RPS5, RPS3, RPS7, RPS25, RPS18, RPL30, RPS19, RPL22, EEF1A1P5, RPLP0, RPL9, RPS10, RPL11, UBB, RPL12, RPS20, RPL10A
GO:0007160 cell-matrix adhesion	**4.53**	14	ITGA11, ITGA1, ACTN1, ITGB5, ITGA3, VTN, ITGB1, CTNNB1, THY1, CD44, ITGAV, ITGA7, RHOA, FN1
GO:0031982 vesicle	**3.07**	81	HSP90AB1, A2M, VAPA, ATP1B3, PDIA3, RAB5B, RAB5C, PDIA6, ANPEP, PDIA4, CLTC, CANX, PRDX1, RABAC1, SLC1A5, COPB2, APOA1, RPN1, DNAJC5, ATP6V0D1, RAB21, BSG, HSP90AA1, ACTN4, ERP29, SLC3A2, ACTN1, MMP14, STOM, IGF2R, DLD, RAB5A, RAB14, CTSD, GNAS, CTSB, ALDOA, CAV2, TF, RAB7A, CAV1, YWHAZ, GANAB, PF4, ITGB1, CALU, ANXA6, CD9, ANXA7, STX12, SYPL1, ECE1, TMED2, ALB, RAC1, RAB11B, TMED10, SEC22B, HSPA5, THBS1, MYOF, HSPA8, FN1, RAB2A, P4HB, ITGA1, GARS, YWHAB, ATP1A1, SPARC, YWHAE, ANXA2, NCSTN, LAMP1, LAMP2, HSP90B1, LRP1, PPIB, TFRC, ANXA11, HSPD1
GO:0016477 cell migration	**3.02**	29	CTHRC1, CAV2, NRP1, ATP5B, ITGA11, PF4, CDH2, ITGB1, APOA1, CD44, RAC1, KRT2, MSN, CAP1, PPAP2A, THBS1, PPAP2B, FN1, ITGA1, MYH9, MMP14, YWHAE, CDH13, ITGA5, CFL1, PDGFRB, VCAN, LAMC1, ENG
GO:0005739 mitochondrion	**2.82**	121	TSPO, STOML2, COX5B, HIBADH, PDHB, UQCR10, CISD1, SLC25A24, LRRC59, DNAJC5, BSG, COX6C, NNT, PTRF, DLD, ATP5C1, MDH2, CAV2, HSD17B10, CAV1, GLUD1, TMX4, SFXN3, HSPA1A, SFXN1, PTRH2, HADHA, HADHB, MTCH2, GSTK1, COX6B1, HSPE1, FH, GPD2, ATP5J2, PHB, GARS, VDAC2, VDAC3, VDAC1, SLC25A11, USMG5, SLC25A13, GLS, NDUFV2, ALDH2, HSPD1, PC, CYB5R3, UQCRC2, ATP5D, UQCRC1, ATP5B, CYC1, PRDX4, PRDX5, PRDX3, UQCRFS1, CLTC, PRDX1, UQCRQ, NDUFS5, P4HA1, NDUFS8, SLC25A3, ATP5L, ATP5O, SLC25A1, CAT, ATP5I, NDUFS3, NDUFS2, ATP5H, NDUFS1, SQRDL, NDUFB10, SLC25A4, SSBP1, SLC25A5, AIFM1, SLC25A6, NDUFC2, NDUFA13, COX4I1, CYB5A, CYB5B, DECR1, NDUFA12, ALDH7A1, ALDH1B1, CTSD, TOMM22, CTSB, OAT, UQCRB, NDUFB4, YWHAZ, ECH1, NDUFB8, NDUFB9, ALDH3A2, HSD17B4, HSPA9, NDUFA4, DLST, SHMT2, COX7A2, NDUFA8, NDUFA9, PSAP, CS, ATP5F1, YWHAE, SOD2, SDHA, SDHB, TFRC, PHB2, ATP5A1, SCP2, MGST1
GO:0031012 extracellular matrix	**2.13**	29	TF, CTHRC1, TNC, HSD17B12, VTN, CALR, AHSG, GPC4, CD44, COL6A3, COL6A2, COL6A1, COL12A1, COL8A1, THBS1, GPC1, FN1, LGALS1, CRTAP, SPARC, MMP14, EMILIN1, ANXA2, FBLN1, LEPRE1, COL1A2, VCAN, COL1A1, LAMC1
GO:0005509 calcium ion binding	**1.91**	59	S100A6, S100A8, ATP5B, PDIA4, PRKCSH, CANX, SSR1, ATP2B1, ATP2B4, GSN, SLC25A24, ASPH, CAPNS1, ACTN4, ACTN1, CCDC47, MMP14, VCAN, FKBP10, MYL6, FKBP9, GALNT2, GALNT1, ITGA11, CDH2, LMAN2, CALR, TPM4, CALU, MYL9, ANXA6, ANXA7, ITGAV, HSPA5, THBS1, GPD2, CACNA2D1, MRC2, ITGA1, ANXA1, S100A11, S100A10, ITGA3, SPARC, MYL12A, ANXA5, ANXA4, ANXA2, CDH13, HSP90B1, FBLN1, SLC25A13, LRP1, ATP2A2, ITGA5, ITGA7, ANXA11, SSR4, SPTAN1

Supplementary Table 9. List of the 31 proteins not detected in min-ECM. Proteins are indicated as Protein IDs and Gene ID-alphabetically ordered.

Protein ID	LFQ nonmin-ECM	LFQ activin-ECM
CON__Q3SZH5	57415000	28079000
REV__Q9Y4K1	4093900000	1631000000
P53680-2	6597400	5505900
O15145	13579000	4813600
O75348	4664900	3853100
CON__Q2UVX4	44973000	29037000
P20674	4369000	4995900
P29279	9471300	4789600
Q9UBR2	5041500	2913600
P26641	4475300	3063200
Q16658	10938000	6265100
P11413	7834100	5142400
Q8N257	48278000	7533500
P98160	7959400	5461300
P14923	333540	656640
Q5T749	7178300	3120300
S4R3I5	11006000	8811500
CON__Q3SZR3	7726200	9361400
P04156-2	27450000	9689700
Q16647	26280000	8205000
P62277	110700000	12213000
P62263	18052000	8274200
P06702	6088700	4419500
CON__Q9N2I2	128160000	39370000
CON__P41361	5447300	4142800
P05121	186970000	47978000
Q15393	14687000	9808800
Q5T8R3	2907700	2875500
P62316	3337000	2068300
G3V5X4	5709600000	4611100000
Q15582	88621000	3922100

Supplementary Table 10. List of the 149 proteins detected only in min-ECM. Proteins are ranked for abundance measured by LFQ.

Protein ID	LFQ min-ECM
Q14195	2182700000
REV__S4R403	2141700000
Q2Y0W8-5	238890000
REV__Q96HY7	120770000
A6NLH6	18780000
Q8N6L1	18651000
P49914-2	17077000
Q4G0P3	16103000
Q6ZUX7	13796000
Q8N5M9	12849000
Q8N1B9	12220000
O95479	12068000
G3V5P8	11530000
Q86YZ3	10818000
Q9BXK5-4	10780000
P00441	10574000
O14828-2	9789300
C9JEN3	9686300
O75083	9418600
P10599	9278300
M0QZY4	9229700
Q06136	8958000
Q8IVL6-2	8793300
Q16134-3	8649100
O14548	8298200
P57105	8210400
Q9H251-5	8006300
P03928	7708100
Q9HB66	7245800
Q86Y39	7206200
Q9BRR6-2	7181400
Q12931-2	7065800
P61006	7016100
P23368	6990500
P41159	6957300
Q6YN16	6808400
H3BSC1	6192000
Q15293	6079000
P53597	6026500
E5RIP4	5875400
Q6UXV4	5868200
REV__Q5JVD3	5728100
H3BR27	5712600
Q9H0R3-2	5534700
Q9H2U2-6	5531400
Q13641	5445600
Q4KMQ2-3	5441400
Q92544	5434500
J3QRU4	5420900
E5RK01	5325400
Q9BUB7-2	5219200
Q9H330-2	5100700
Q5T123	5066700
Q9Y696	4916100
O75955	4896500
CON__P07224	4780100
P28066	4755600
K7ENI6	4695400
REV__Q86VH2-3	4609900
O00161-2	4530900
Q6P587	4158800
B4DLH2	4016200
J3QL56	3718600
Q15155	3625800
Q8NBJ5	3509300
Q96CS3	3428400
Q92633	3359000
REV__CON__P02672	3299100
REV__M0R0Q7	3204700
Q5XKP0	3113500
O95573	3056700
Q6IAK0	2986900
F8WAS3	2924500
P03897	2867200
O96011-2	2835500
O95571	2821200
Q9Y5J7	2804800
Q9Y305-3	2797900
P81605	2745100
Q5JX45	2685900
Q9Y584	2672300
REV__H7C388	2589800
C9JGJ9	2506200
P84095	2483300
B4DQ51	2477000
B4DN67	2419500
E9PCB6	2360500
Q9BW60	2319700
C9JL85	2243300
Q9H3H5-3	2128500
D6RBS5	2085000
Q969M3	2033200
S4R3U9	1997700
F8VQW8	1971000
H0Y8Z9	1968300
S4R329	1949800
G3V5T4	1945800
A8MT40	1884900
Q14739	1765900
Q5T7F5	1696100
P01034	1694200
P23786	1668200
Q9Y320-2	1584300
Q9BRK3-3	1578300
Q9HBH5	1549900
O14521-2	1548900
F5H261	1489700
H0YLB6	1467000
O15438	1397200
Q96QK1	1378900
H0YHJ8	1368200
Q9UM54-5	1353500
REV__Q5T4B2-2	1294900
F5H5N1	1294400
Q9UGQ3-2	1262200
Q6UWP7-3	1252400
P08842	1214400
Q8WVX3	1185500
Q9P0J1	1185500
F8WAX7	1178700
I3L1T3	1145400
Q8NFQ8	1129500
H0YC95	1110600
Q6TDP4	1105600
E9PP42	1079000
C0H5Y7	1041700
O94911	1034600
U3KQU4	1007600
F5H459	970120
B5MCE2	920620
P08473	910030
C9JY28	903360
K7EP56	890940
P52815	859090
Q9NZ08	854950
H7BXK9	829150
M0R1E0	822350
P00156	806720
H7C613	787170
Q5T3Q7	780680
H7BXL1	768380
F5H4N4	662750
E9PSI1	642460
D6RF69	490670
O75051	464780
P05771	461470
H7BYE5	456700
H0YNE5	332980
Q7KYR7-6	284500

REFERENCES

1. Hynes, R.O., *The extracellular matrix: not just pretty fibrils.* Science, 2009. 326(5957): p. 1216-9.
2. Mouw, J.K., G. Ou, and V.M. Weaver, *Extracellular matrix assembly: a multiscale deconstruction.* Nat Rev Mol Cell Biol, 2014. 15(12): p. 771-85.
3. Guilak, F., et al., *Control of stem cell fate by physical interactions with the extracellular matrix.* Cell Stem Cell, 2009. 5(1): p. 17-26.
4. Discher, D.E., D.J. Mooney, and P.W. Zandstra, *Growth factors, matrices, and forces combine and control stem cells.* Science, 2009. 324(5935): p. 1673-7.
5. Reilly, G.C. and A.J. Engler, *Intrinsic extracellular matrix properties regulate stem cell differentiation.* J Biomech, 2010. 43(1): p. 55-62.
6. Sommerfeldt, D.W. and C.T. Rubin, *Biology of bone and how it orchestrates the form and function of the skeleton.* Eur Spine J, 2001. 10 Suppl 2: p. S86-95.
7. Alford, A.I. and K.D. Hankenson, *Matricellular proteins: Extracellular modulators of bone development, remodeling, and regeneration.* Bone, 2006. 38(6): p. 749-57.
8. Marie, P.J., *Bone cell-matrix protein interactions.* Osteoporos Int, 2009. 20(6): p. 1037-42.
9. Badylak, S.F., D.O. Freytes, and T.W. Gilbert, *Extracellular matrix as a biological scaffold material: Structure and function.* Acta Biomater, 2009. 5(1): p. 1-13.
10. Benders, K.E., et al., *Extracellular matrix scaffolds for cartilage and bone regeneration.* Trends Biotechnol, 2013. 31(3): p. 169-76.
11. Caplan, A.I., *Review: mesenchymal stem cells: cell-based reconstructive therapy in orthopedics.* Tissue Eng, 2005. 11(7-8): p. 1198-211.
12. Mauney, J.R., V. Volloch, and D.L. Kaplan, *Role of adult mesenchymal stem cells in bone tissue engineering applications: current status and future prospects.* Tissue Eng, 2005. 11(5-6): p. 787-802.
13. Fitzpatrick, L.E. and T.C. McDevitt, *Cell-derived matrices for tissue engineering and regenerative medicine applications.* Biomater Sci, 2015. 3(1): p. 12-24.
14. Lu, H., et al., *Cultured cell-derived extracellular matrix scaffolds for tissue engineering.* Biomaterials, 2011. 32(36): p. 9658-66.
15. Papadimitropoulos, A., et al., *Engineered decellularized matrices to instruct bone regeneration processes.* Bone, 2015. 70: p. 66-72.
16. Mauney, J.R., D.L. Kaplan, and V. Volloch, *Matrix-mediated retention of osteogenic differentiation potential by human adult bone marrow stromal cells during ex vivo expansion.* Biomaterials, 2004. 25(16): p. 3233-43.
17. Datta, N., et al., *Effect of bone extracellular matrix synthesized in vitro on the osteoblastic differentiation of marrow stromal cells.* Biomaterials, 2005. 26(9): p. 971-7.
18. Prewitz, M.C., et al., *Tightly anchored tissue-mimetic matrices as instructive stem cell microenvironments.* Nat Methods, 2013. 10(8): p. 788-94.
19. Chen, X.D., et al., *Extracellular matrix made by bone marrow cells facilitates expansion of marrow-derived mesenchymal progenitor cells and prevents their differentiation into osteoblasts.* J Bone Miner Res, 2007. 22(12): p. 1943-56.
20. Lai, Y., et al., *Reconstitution of marrow-derived extracellular matrix ex vivo: a robust culture system for expanding large-scale highly functional human mesenchymal stem cells.* Stem Cells Dev, 2010. 19(7): p. 1095-107.

21. Ng, C.P., et al., *Enhanced ex vivo expansion of adult mesenchymal stem cells by fetal mesenchymal stem cell ECM.* Biomaterials, 2014. 35(13): p. 4046-57.
22. Hoshiba, T., et al., *Development of stepwise osteogenesis-mimicking matrices for the regulation of mesenchymal stem cell functions.* J Biol Chem, 2009. 284(45): p. 31164-73.
23. Eijken, M., et al., *The activin A-follistatin system: potent regulator of human extracellular matrix mineralization.* FASEB J, 2007. 21(11): p. 2949-60.
24. Alves, R.D., et al., *Activin A suppresses osteoblast mineralization capacity by altering extracellular matrix (ECM) composition and impairing matrix vesicle (MV) production.* Mol Cell Proteomics, 2013. 12(10): p. 2890-900.
25. Bruedigam, C., et al., *Basic techniques in human mesenchymal stem cell cultures: differentiation into osteogenic and adipogenic lineages, genetic perturbations, and phenotypic analyses.* Curr Protoc Stem Cell Biol, 2011. Chapter 1: p. Unit1H 3.
26. Morhayim, J., et al., *Proteomic signatures of extracellular vesicles secreted by nonmineralizing and mineralizing human osteoblasts and stimulation of tumor cell growth.* FASEB J, 2015. 29(1): p. 274-85.
27. Huang da, W., B.T. Sherman, and R.A. Lempicki, *Systematic and integrative analysis of large gene lists using DAVID bioinformatics resources.* Nat Protoc, 2009. 4(1): p. 44-57.
28. Ehlen, H.W., et al., *Inactivation of anoctamin-6/Tmem16f, a regulator of phosphatidylserine scrambling in osteoblasts, leads to decreased mineral deposition in skeletal tissues.* J Bone Miner Res, 2013. 28(2): p. 246-59.
29. Anderson, H.C., R. Garimella, and S.E. Tague, *The role of matrix vesicles in growth plate development and biomineralization.* Front Biosci, 2005. 10: p. 822-37.
30. Kearns, A.E., et al., *Cloning and characterization of a novel protein kinase that impairs osteoblast differentiation in vitro.* J Biol Chem, 2001. 276(45): p. 42213-8.
31. Schinke, T., et al., *The serum protein alpha2-HS glycoprotein/fetuin inhibits apatite formation in vitro and in mineralizing calvaria cells. A possible role in mineralization and calcium homeostasis.* J Biol Chem, 1996. 271(34): p. 20789-96.
32. Denecke, B., et al., *Tissue distribution and activity testing suggest a similar but not identical function of fetuin-B and fetuin-A.* Biochem J, 2003. 376(Pt 1): p. 135-45.
33. Johnson, K., et al., *Matrix vesicle plasma cell membrane glycoprotein-1 regulates mineralization by murine osteoblastic MC3T3 cells.* J Bone Miner Res, 1999. 14(6): p. 883-92.
34. Salasznyk, R.M., et al., *Adhesion to Vitronectin and Collagen I Promotes Osteogenic Differentiation of Human Mesenchymal Stem Cells.* J Biomed Biotechnol, 2004. 2004(1): p. 24-34.
35. Mackie, E.J. and S. Ramsey, *Modulation of osteoblast behaviour by tenascin.* J Cell Sci, 1996. 109 (Pt 6): p. 1597-604.
36. Ogura, N., et al., *Differentiation of the human mesenchymal stem cells derived from bone marrow and enhancement of cell attachment by fibronectin.* J Oral Sci, 2004. 46(4): p. 207-13.
37. Allori, A.C., A.M. Sailon, and S.M. Warren, *Biological basis of bone formation, remodeling, and repair-part II: extracellular matrix.* Tissue Eng Part B Rev, 2008. 14(3): p. 275-83.
38. Raaijmakers, M.H., et al., *Bone progenitor dysfunction induces myelodysplasia and secondary leukaemia.* Nature, 2010. 464(7290): p. 852-7.
39. Zambetti, N.A., et al., *Mesenchymal Inflammation Drives Genotoxic Stress in Hematopoietic Stem Cells and Predicts Disease Evolution in Human Pre-leukemia.* Cell Stem Cell, 2016. 19(5): p. 613-627.
40. Gubbiotti, M.A., T. Neill, and R.V. Iozzo, *A current view of perlecan in physiology and pathology: A mosaic of functions.* Matrix Biol, 2016.

41. Lowe, D.A., et al., *Deficiency in perlecan/HSPG2 during bone development enhances osteogenesis and decreases quality of adult bone in mice.* Calcif Tissue Int, 2014. 95(1): p. 29-38.
42. Izu, Y., et al., *Type XII collagen regulates osteoblast polarity and communication during bone formation.* J Cell Biol, 2011. 193(6): p. 1115-30.